

<https://doi.org/10.15388/vu.thesis.486>

<https://orcid.org/0000-0003-1204-6770>

VILNIUS UNIVERSITY

CENTER FOR PHYSICAL SCIENCES AND TECHNOLOGY

Povilas Virbickas

Development of Sensors and Biosensors Based on Prussian Blue and Cobalt Hexacyanoferrate

DOCTORAL DISSERTATION

Natural Sciences,
Chemistry (N 003)

VILNIUS 2023

This dissertation was written between 2019 and 2023 in Vilnius University, Faculty of Chemistry and Geosciences, Institute of Chemistry.

Academic supervisor – Prof. Dr. Aušra Valiūnienė (Vilnius University, Natural sciences, chemistry – N 003).

Dissertation Defence Panel:

Chairman – Prof. Dr. Almira Ramanavičienė (Vilnius University, Natural Sciences, Chemistry – N 003).

Members:

Dr. Marius Dagys (Vilnius University, Natural Sciences, Biochemistry – N 004);

Prof. Dr. Tautgirdas Ruzgas (Molmo University, Natural Sciences, Biochemistry – N 004);

Prof. Dr. Gintaras Valinčius (Research Council of Lithuania, Natural Sciences, Biochemistry – N 004);

Prof. Dr. Vida Vičkačkaitė (Vilnius University, Natural Sciences, Chemistry – N 003).

The dissertation is defended at a public meeting of the Dissertation Defence Panel at 14:00 on 29 September 2023 at the Inorganic Chemistry Auditorium of the Institute of Chemistry, Vilnius University. Address: Naugarduko str. 24, LT-03225, Vilnius, Lithuania, tel. +370 5 219 3105; e-mail: info@chgf.vu.lt

The text of this dissertation can be accessed at the library of Vilnius University and at the library of Center for Physical Sciences and Technology, as well as on the website of Vilnius University: <https://www.vu.lt/naujienos/ivykiu-kalendorius>

<https://doi.org/10.15388/vu.thesis.486>

<https://orcid.org/0000-0003-1204-6770>

VILNIAUS UNIVERSITETAS
FIZINIŲ IR TECHNOLOGIJOS MOKSLŲ CENTRAS

Povilas Virbickas

Berlyno mėlynojo ir kobalto heksacianoferato taikymas formuojant cheminius ir biologinius jutiklius

DAKTARO DISERTACIJA

Gamtos mokslai,
Chemija (N 003)

VILNIUS 2023

Disertacija rengta 2019 - 2023 metais Vilniaus universiteto Chemijos ir geomokslų fakulteto Chemijos institute.

Mokslinė vadovė – prof. dr. Aušra Valiūnienė (Vilniaus universitetas, gamtos mokslai, chemija – N 003).

Gynimo taryba:

Pirmininkė – prof. dr. Almira Ramanavičienė Vilniaus universitetas, gamtos mokslai, chemija – N 003).

Nariai:

dr. Marius Dagys (Vilniaus universitetas, gamtos mokslai, biochemija – N 004);

prof. dr. Tautgirdas Ruzgas (Malmės universitetas, gamtos mokslai, biochemija – N 004);

prof. dr. Gintaras Valinčius (Lietuvos mokslo taryba, gamtos mokslai, biochemija – N 004);

prof. dr. Vida Vičkačkaitė (Vilniaus universitetas, gamtos mokslai, chemija – N 003).

Disertacija ginama viešame Gynimo tarybos posėdyje 2023 m. rugsėjo mėn. 29 d. 14 val., Vilniaus universiteto Chemijos instituto Neorganinės chemijos auditorijoje. Adresas: Naugarduko g. 24, LT-03225, Vilnius, Lietuva, tel +370 5 219 3105; el. paštas: info@chgf.vu.lt

Disertaciją galima peržiūrėti Vilniaus universiteto, Fizinių ir technologijos mokslų centro bibliotekose ir VU interneto svetainėje adresu: <https://www.vu.lt/naujienos/ivykiu-kalendorius>

LIST OF ORIGINAL PAPERS

- Paper 1** P. Virbickas, A. Valiūnienė, A. Ramanavičius. Towards electrochromic ammonium ion sensors. *Electrochem. Commun.* 94 (2018) 41–44.
- Paper 2** A. Valiūnienė, P. Virbickas, G. Medvikytė, A. Ramanavičius. Urea Biosensor Based on Electrochromic Properties of Prussian Blue. *Electroanalysis* 32 (2020) 503–509.
- Paper 3** P. Virbickas, G. Kavaliauskaitė, A. Valiūnienė, V. Plaušinitienė, A. I. Rekertaitė, A. Ramanavičius. Cobalt hexacyanoferrate based optical sensor for continuous optical sensing of hydrogen peroxide. *Electrochim. Acta* 362 (2020) 137202.
- Paper 4** P. Virbickas, G. Žižiūnaitė, A. Ramanavičius, A. Valiūnienė. Prussian Blue Modified Amperometric Hg^{2+} Ion Biosensor Based on Glucose Oxidase Inhibition. *Electroanalysis* 34 (2022).

AUTHOR'S CONTRIBUTION TO THE ORIGINAL PAPERS

- Paper 1** Planned and performed the investigations of the electrochromic ammonium ion sensor, analysed obtained data, prepared the original draft of the paper.
- Paper 2** Planned the experiments, participated in investigations of the electrochromic urea biosensor, analysed obtained data, prepared the original draft of the paper.
- Paper 3** Participated in planning and performing cyclic voltammetry and absorption spectroscopy-based investigations of the cobalt hexacyanoferrate-based hydrogen peroxide sensor, participated in interpreting obtained data, participated in writing the paper.
- Paper 4** Planned the experiments, participated in performing investigations of the amperometric Hg^{2+} ion biosensor, participated in interpreting obtained data, participated in writing the paper.

CONFERENCES

1. **P. Virbickas**, A. Valiūnienė. Elektrochrominis amonio jonų jutiklis. "Chemija ir cheminė technologija", May 17, 2019, Vilnius, Lithuania. ISBN 978-609-07-0176-8, pp. 316 – 320. Oral presentation.
2. **P. Virbickas**, G. Kavaliauskaitė, A. Valiūnienė. Application of transition metals hexacyanoferrates in optical sensing of hydrogen peroxide. "Nanostructured Bioceramic Materials 2020", December 1 – 3, 2020, Vilnius, Lithuania. ISBN 978-609-07-0557-5, p. 77. Poster presentation.
3. **P. Virbickas**, A. Valiūnienė, G. Kavaliauskaitė, G. Žižiūnaitė. The applications of Prussian blue in pH sensing. "OpenReadings 2021", March 16 – 19, 2021, Vilnius, Lithuania. ISBN 978-609-07-0590-2, p. 420. Poster presentation.
4. **P. Virbickas**, N. Dėnas, A. Valiūnienė, G. Kavaliauskaitė. Application of Prussian blue in the development of enzymatic biosensors. "Chemistry and Chemical Technology 2021", September 24, 2021, Vilnius, Lithuania. P. 27. Poster presentation.
5. **P. Virbickas**, G. Žižiūnaitė, A. Valiūnienė. Prussian blue-based electrochemical biosensor for Hg^{2+} ions. "OpenReadings 2022", March 15 – 18, Vilnius, Lithuania. DOI: TBA, p. 371. Poster presentation.
6. **P. Virbickas**, G. Žižiūnaitė, A. Valiūnienė. Glucose oxidase inhibition-based Hg^{2+} ion biosensor. "Chemistry and Chemical Technology 2023", March 10, 2023, Vilnius, Lithuania. ISBN 978-609-07-0833-0, p. 126. Poster presentation.

LIST OF ABBREVIATIONS

λ_{max}	Wavelength corresponding to optical absorption maximum
BG	Berlin green
CoHCF	Cobalt hexacyanoferrate
CoHCF _{ox}	Cobalt hexacyanoferrate at oxidised oxidation state
CoHCF _{red}	Cobalt hexacyanoferrate at reduced oxidation state
dj	Change in value of current
EDS	Energy-dispersive X-ray spectrometry
EDTA	Ethylenediaminetetraacetic acid
FTO	Fluorine doped tin oxide
GI-XRD	Grazing incidence X-ray diffraction
GOx	Glucose oxidase
ITO	Indium-tin oxide
NiHCF	Nickel hexacyanoferrate
PB	Prussian blue
PBS	Phosphate-buffered solution
PBSA	Prussian blue structural analogues
PW	Prussian white
PY	Prussian yellow
SEM	Scanning electron microscopy
u.a.	Absorption units
XRD	X-ray diffraction
ΔA	Change in value of optical absorption maximum

TABLE OF CONTENTS

INTRODUCTION.....	11
1. LITERATURE REVIEW.....	14
1.1. Chemical composition and electrochemical properties of Prussian blue and its structural analogues.....	14
1.2. Applications of Prussian blue and its structural analogues in chemical analysis.....	16
1.2.1. Sensitivity of PB (and PBSA) to compounds with oxidising or reducing properties.....	16
1.2.2. Dependence of the electrochemical properties of PB and PBSA on the pH value and the concentration of reduction-promoting ions.....	18
1.2.3. Dependency of PB optical properties on pH.....	19
2. EXPERIMENTAL.....	21
2.1. Materials.....	21
2.2. Equipment for electrochemical and optical investigations.....	21
2.3. Deposition of PB and CoHCF layers.....	21
2.4. Immobilisation of enzymes on a PB layer.....	23
2.5. Investigation of the electrochromic ammonium ion sensor (glass ITO PB electrode).....	23
2.6. Investigation of the electrochromic urea biosensor (glass ITO PB urease).....	24
2.7. Investigation of CoHCF-based optical H ₂ O ₂ sensor.....	24
2.8. Investigation of the amperometric Hg ²⁺ ion biosensor (glass FTO PB GOx).....	25
3. RESULTS AND DISCUSSION.....	26
3.1. Investigation of the electrochromic ammonium ion sensor (glass ITO PB electrode).....	26
3.1.1. Electrochemical stabilisation of a PB layer.....	26
3.1.2. Investigation of the electrochromic response of the glass ITO PB electrode to ammonium ions.....	27

3.2. Investigation of the electrochromic urea biosensor (glass ITO PB urease).....	30
3.2.1. Investigation of the glass ITO PB urease biosensor in urea-containing PBS.....	30
3.2.2. Evaluation of pH influence on the optical properties of the glass ITO PB urease biosensor.....	34
3.3. Investigation of the optical CoHCF-based sensor for hydrogen peroxide.....	36
3.3.1. Investigation of electrochemical and electrochromic properties of CoHCF.....	36
3.3.2. The impact of O ₂ on the optical properties of CoHCF _{ox}	40
3.3.3. Investigation of the optical H ₂ O ₂ sensor (glass ITO CoHCF _{ox} KCl _{cycled} electrode) in the hydrogen peroxide-containing solution.....	41
3.4. Investigation of the PB-modified amperometric Hg ²⁺ ion biosensor based on glucose oxidase inhibition (glass FTO PB GOx).....	44
3.4.1. The principle of the glass FTO PB GOx biosensor operation.....	44
3.4.2. Optimisation of potentiostatic conditions.....	44
3.4.3. Amperometric investigation of the glass FTO PB GOx biosensor.....	46
GENERAL CONCLUSIONS.....	50
REFERENCES.....	51
SANTRAUKA.....	55
ACKNOWLEDGEMENT.....	70
CURRICULUM VITAE.....	71

INTRODUCTION

Prussian blue (PB) and its structural analogues (PBSA), e.g., cobalt hexacyanoferrate (CoHCF), are inorganic pigments often applied in construction of sensors and biosensors. Some of the main advantages of PB and PBSA are the low cost of these materials and the low potential ($\sim 0 \text{ V vs Ag|AgCl, KCl}_{\text{sat}}$) of working electrode required for the operation of PB-based sensors. The low potential of a working electrode ($\sim 0 \text{ V vs Ag|AgCl, KCl}_{\text{sat}}$) used during sensor operation is a particularly useful feature, reducing the risk of interfering oxidation of other electrochemically active species that may be present in the analysed sample.

The determination of ammonium ions (or ammonia), Hg^{2+} ions, urea and hydrogen peroxide concentrations are important in both clinical analysis and environmental monitoring. However, despite the potential effectiveness of PB and PBSA in improving the performance of analytical techniques, there have been no studies to date investigating the applicability of PB for the electrochromic determination of ammonium ions and urea, the suitability of PB for the detection of heavy metal ions (e.g., Hg^{2+}) through the enzyme inhibition and the applicability of CoHCF for the optical detection of hydrogen peroxide. Moreover, application of PB and/or PBSA for the aforementioned analytical purposes (detection of hydrogen peroxide, ammonium ion, urea, heavy metal ions) could potentially improve the characteristics of existing analytical systems, e.g.: (i) expand the limits of the determined concentrations, (ii) ensure greater selectivity of the sensor to the analyte in the presence of other electrochemically active substances in the analysed sample, (iii) increase the inertness of the sensor towards factors such as the buffer capacity of the sample or the oxidising effect of oxygen.

The aim of this study:

To develop Prussian blue-based and/or cobalt hexacyanoferrate-based sensors for detection of ammonium ion, urea, hydrogen peroxide and Hg^{2+} ion.

The objectives of this study:

1. To form an electrochromic ammonium ion sensor by coating the glass/ITO electrode with a PB layer; to investigate electrochromic response of the developed sensor towards different concentrations of ammonium ions in solution.

2. To form an electrochromic urea biosensor by coating a glass|ITO electrode with a PB layer and immobilising an enzyme urease (glass|ITO|PB|urease); to investigate electrochromic response of the biosensor to different concentrations of urea in solution.
3. To develop an optical hydrogen peroxide sensor by coating a glass|ITO electrode with a CoHCF_{ox} layer; to select optimal conditions for monitoring the electrochromic transition between CoHCF_{ox} and CoHCF_{red}; to investigate the optical response of the developed sensor to different concentrations of hydrogen peroxide in solution.
4. To form an electrochemical Hg²⁺ ion sensor based on inhibition of glucose oxidase (GOx) by covering the glass|FTO electrode with a PB layer (glass|FTO|PB) and immobilising GOx (glass|FTO|PB|GOx); to determine the optimal potential for the operation of the developed biosensor; to investigate amperometric response of the developed biosensor to different concentrations of Hg²⁺ ions in solution.

Scientific novelty:

In order to improve the characteristics of chemical and biological sensors, such as selectivity of the analysis and linear range of concentrations, a lot of research has been done on improving the composition of sensors and testing new materials for the detection of analytes. An example of this research is Prussian blue (PB) related studies: PB was first used in a field of chemical analysis due to its sensitivity to hydrogen peroxide, however, later applications of PB have expanded to electrochemical detection of ions, optical and electrochemical detection of pH changes, electrochemical detection of ascorbic acid, and other applications. Structural analogues of PB, such as Co and Ni hexacyanoferrates, have also received considerable scientific attention – these materials have been used for electrochemical determination of hydrogen peroxide, as well as for increasing the durability and stability of PB coatings.

In this work, PB was used for the first time for the electrochromic determination of ammonium ions and urea concentration, as well as for the electrochemical determination of Hg²⁺ ions concentration. Meanwhile, a structural analogue of PB, cobalt hexacyanoferrate (CoHCF), was used for the first time for the optical determination of hydrogen peroxide. The main scientific and practical achievements of this work are:

1. It was demonstrated that PB can be applied in electrochromic detection of ammonium ion, and urease-modified PB can be used for the electrochromic determination of urea.
2. Measurement of urea concentration by the “soluble” PB-containing glass|ITO|PB|urease biosensor was found to be independent of alkaline hydrolysis of the PB coating, making the glass|ITO|PB|urease sensor less sensitive to changes in the buffer capacity of the analysed sample than previously developed “insoluble” PB-based urea biosensors.
3. The structural analogue of PB – CoHCF – was used for the first time for the optical determination of hydrogen peroxide. It was confirmed that optical properties of CoHCF_{ox} are resistant to the impact of oxygen from air. This feature of CoHCF has a great importance, since the reduced form of PB – Prussian white – which was used for the optical determination of hydrogen peroxide during previous investigations, can be affected by oxygen from air or solution, resulting in reduced selectivity of Prussian white layer towards hydrogen peroxide.
4. For the first time, PB was applied in amperometric determination of Hg²⁺ ions concentration via glucose oxidase inhibition. Due to the use of PB in a construction of biosensor, biosensor formed in this work was operating at relatively low potential of +0.2 V vs Ag|AgCl, KCl_{sat} that is significantly lower than +0.4 V – +0.7 V (vs Ag|AgCl, KCl_{sat}) potentials used in operation of earlier developed amperometric glucose oxidase inhibition-based Hg²⁺ ion biosensors. This finding is important because low electrode potential enables to avoid some electrochemical oxidation reactions of other compounds present in the sample consequently increasing the reliability of the analysis.

Statements for defence:

1. Prussian blue can be applied in electrochromic determination of ammonium ions concentration.
2. The biosensor formed by coating a glass|ITO electrode with a layer of Prussian blue and immobilising an enzyme urease can be used for the electrochromic determination of urea concentration.
3. Cobalt hexacyanoferrate can be applied in optical determination of hydrogen peroxide.
4. The biosensor formed by coating a glass|FTO electrode with a layer of Prussian blue and immobilising an enzyme glucose oxidase can be used for amperometric determination of Hg²⁺ ions concentration.

1. LITERATURE REVIEW

1.1. Chemical composition and electrochemical properties of Prussian blue and its structural analogues

In order to overview possible ways of applying Prussian blue (PB) and its structural analogues (PBSA) in chemical analysis, it is important to look over possible chemical compositions of these compounds and to evaluate the impact of PB and/or PBSA chemical composition on electrochemical (and electrochromic) properties of these materials. PB has a cubic crystal lattice, however, chemical formula of PB differs depending on amount Fe^{3+} ions in the crystal lattice of PB [1]. PB can be present in the so-called “soluble” form, in which a part of Fe^{3+} ions is replaced by other ions which supports charge neutrality during PB reduction process (e.g., K^+ , Rb^+ and NH_4^+ ions), or “insoluble” form, in which Fe^{3+} ions are not replaced by other ions [1-4]. Taking into account that both “soluble” and “insoluble” forms of PB are actually insoluble in water, the terms “soluble” and “insoluble” PB are used to distinguish the ability of PB to form a suspension [5]. Chemical formulas of the “soluble” and “insoluble” PB can be described as $\text{XFe}^{\text{III}}[\text{Fe}^{\text{II}}(\text{CN})_6]$ (where X is monovalent cation, e.g., K^+ and NH_4^+) and $\text{Fe}_4^{\text{III}}[\text{Fe}^{\text{II}}(\text{CN})_6]_3$, respectively [1-4].

PB and some PBSA (e.g., Co, Ni hexacyanoferrates) are electrochromic materials [6-8]. PB can be chemically or electrochemically transformed between different oxidation states, exhibiting different colours - PB can be reduced into its optically transparent form “Prussian white” (PW), or it can be oxidised into yellow-coloured oxidised state named as “Prussian yellow” (PY) [6,9]. Moreover, transitional states between PW, PB and PY are also possible, e.g., PB can be oxidised into green-coloured state between PB and PY – this compound is named as “Berlin green” [6]. Chemical formulas of “soluble” and “insoluble” PW can be described as $\text{X}_2\text{Fe}^{\text{II}}[\text{Fe}^{\text{II}}(\text{CN})_6]$ and $\text{X}_4\text{Fe}_4^{\text{II}}[\text{Fe}^{\text{II}}(\text{CN})_6]_3$, while formulas of PY can be written as $\text{Fe}^{\text{III}}[\text{Fe}^{\text{III}}(\text{CN})_6]$ and $\text{Fe}_4^{\text{III}}[\text{Fe}^{\text{III}}(\text{CN})_6]_3(\text{A})_3$ (where X is PB reduction-promoting ion, A – monovalent anion), correspondingly [2,4,10,11]. It is important to note that there are some confusion in scientific literature about the names of different oxidation states of PB, e.g., the compound with formula $\text{Fe}_4^{\text{III}}[\text{Fe}^{\text{III}}(\text{CN})_6]_3(\text{A})_3$ sometimes is called both PY or BG [10,12]. Furthermore, whether the “soluble” form of PB can be converted to the PY form depends on the type of ion intercalated in the PB crystal lattice, e.g., K^+ ion-containing PB can be oxidised to BG (or PY), while Rb^+ or NH_4^+ ion-

containing PB cannot be oxidised to higher oxidation states [4,11]. Other PBSA (e.g., Co, Ni hexacyanoferrates) also have different colours at different oxidation states, e.g., “regular” Co hexacyanoferrate is green at reduced state and purple in oxidised state [7,13], while Ni hexacyanoferrate changes its colour from transparent to yellow when it is transformed from reduced to oxidised state in K^+ -containing solution [14].

Considering that application of PB (and PBSA) in chemical analysis often involves transitions between different oxidation states of PB, it is important to ensure that PB is electrochemically stable, i.e. it can be reduced (or oxidised) and then transformed back to its initial oxidation state multiple times. By investigating redox transitions between PB and PY, it was determined that “soluble” PB exhibits better electrochemical stability than “insoluble” PB [15,16]. Moreover, it was also proposed that “insoluble” PB is transformed into “soluble” form under conditions of potential cycling between PW and PB forms and the presence of PB reduction-promoting ions in solution [3,17]. Therefore, in order to ensure better electrochemical stability of PB and to ensure that the transition between “insoluble” and “soluble” PB forms will not occur spontaneously during exploitation of PB-based sensing system, “soluble” form of PB seems to be more advantageous in analytic purposes, especially if redox transition is required for the PB-based sensing system to operate.

In similarity to PB, electrochemical properties of some PBSA (e.g., Co and Ni hexacyanoferrates) are also dependent on the presence (or the amount) of other cations in the crystal lattice. For example, Co hexacyanoferrate (CoHCF) is considered to be electrochemically active only if reduction-promoting ion (e.g., Li^+ , Na^+ , K^+) is presented in its crystal lattice [7,13]. Therefore, CoHCF having formula [7,13] $X_2Co^{II}[Fe^{II}(CN)_6]$ (where “X” - Li^+ , Na^+ , K^+) seems to be more promising for electroanalytical (and electrochromic) applications than inserted cation-free form of CoHCF ($Co_2^{II}[Fe^{II}(CN)_6]$). Meanwhile, reduction potential of Ni hexacyanoferrate (NiCoHCF) is dependent on the amount of other cations (besides Ni^{2+}) in the crystal lattice: it was reported [18] that NiHCF forms having larger amount of K^+ counterions inserted to the crystal lattice tend to produce voltammetric peaks at more positive potentials. Summarising these facts, it can be concluded that the chemical composition of PB and PBSA (in particular – an amount of counterions in the crystal lattice) has a significant impact on their electrochemical properties.

1.2. Applications of Prussian blue and its structural analogues in chemical analysis

Prussian blue (PB) and its structural analogues (PBSA) are often applied in a field of chemical analysis – these compounds are used in developing sensors and biosensors for glucose [19-21], hydrogen peroxide [21-23], urea [24], ascorbic acid [25,26], cholesterol [27,28], nucleic acids [29], etc [23,30]. In often case applications of PB (and PBSA) in chemical analysis is based on following properties of PB (and PBSA):

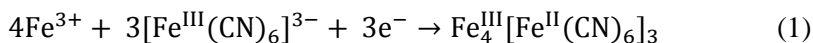
- 1) PB (and PBSA) reacts with some substances exhibiting oxidising or reducing properties;
- 2) Reduction potential of PB (and PBSA) depends on the concentration of reduction-promoting ions in the solution; charge transfer resistance of PB films is dependent on pH.
- 3) In some cases, optical properties of PB can be dependent on pH of the solution as well.

1.2.1. Sensitivity of PB (and PBSA) to compounds with oxidising or reducing properties

Perhaps the most commonly used property of PB in sensorics is reactions of PB with compounds exhibiting oxidising or reducing properties, e.g., ascorbic acid and hydrogen peroxide [23,24,26,31]. When PB reacts with ascorbic acid, PB is reduced to its colourless form - Prussian white (PW) [26]. Meanwhile, the sensitivity of PB to hydrogen peroxide is based on chemical reaction between reduced form of PB (PW) and H_2O_2 – colourless PW reacts with H_2O_2 by forming deep blue-coloured PB [24,31,32]. Because of this H_2O_2 -caused change in colour, PW can be used for the optical determination of H_2O_2 [24,31,32]. However, optical determination of H_2O_2 using PW has a drawback - PW can be oxidised into PB not only due to reaction with hydrogen peroxide, but also due to the oxidising influence of oxygen presented in air or solution [31,33,34]. This interaction between PW and oxygen can potentially reduce the reliability of optical H_2O_2 detection [34].

The reactivity of PW in the reaction with oxygen is related to the size of PW crystals – it was found by investigating hydrothermally synthesized PW crystals that crystals larger than 1 μm in size are not oxidised by oxygen presented in air or solution [31,35]. Meanwhile, PW crystals smaller than 1 μm can be oxidised by oxygen easily [31]. Thus, relatively big (at least 1 μm)

PW crystals can be applied in reliable optical detection of hydrogen peroxide [31]. Another approach to PB (or PW) synthesis is an electrochemical deposition from a solution containing Fe^{3+} and $[\text{Fe}^{\text{III}}(\text{CN})_6]^{3-}$ ions (Eq. 1) [10,34,36]. Electrochemical deposition of PW and PB coatings on conductive substrates seems to be advantageous, since electrochemically formed PW or PB crystals are attached to the surface of the substrate and no immobilisation procedures are needed [10,34,36].



Previous investigations have indicated that both electrochemically and chemically formed PW coatings can be successfully applied in direct optical detection of hydrogen peroxide and/or detection of hydrogen peroxide formed during catalytic oxidation of glucose [24,32,34]. However, both chemically and electrochemically formed PW coatings have been reported to be sensitive to oxygen [31,32,34], that may affect the reliability of hydrogen peroxide detection. On the purpose to improve the resistance of optical hydrogen peroxide determination systems to the oxidative impact of oxygen, other metal hexacyanoferrates, e.g., cobalt hexacyanoferrate (CoHCF), could be considered as the alternative to conventional ferric hexacyanoferrate (PB). Even though CoHCF does not catalyse reduction of hydrogen peroxide in such way as it is catalysed by PW, CoHCF shows electrocatalytic activity towards electrochemical oxidation of hydrogen peroxide [37,38]. The catalytic activity of CoHCF, which induces electrochemical hydrogen peroxide oxidation, makes CoHCF coating possibly applicable in optical sensing of hydrogen peroxide because CoHCF coating at oxidised state (CoHCF_{ox}) can be possibly reduced when it reacts with hydrogen peroxide. Nevertheless, as the oxidising agent – CoHCF_{ox} – should be inert towards the oxidising properties of oxygen, therefore, optical detection of hydrogen peroxide using CoHCF_{ox} should be protected from the impact of oxygen.

Chemical reactions between PB (or PBSA) and redox-active substances could be used not only in developing of optical detection techniques, but also for creating electrochemical sensors and biosensors [10,36]. PB is considered as the most advantageous transducer for electrochemical reduction of hydrogen peroxide since the catalytic activity of PB is >1000 higher compared to conventional Pt electrodes [36]. It is worth to mention that PB exhibits electrocatalytic activity in hydrogen peroxide reduction only if PB is converted into reduced form (PW) which is chemically reactive towards H_2O_2 [10,36,39]. This conversion of PB to PW is usually

fulfilled by applying potential of approx. 0 V (*vs* Ag|AgCl, KCl_{sat}) to the PB-covered working electrode [10]. Furthermore, low potential (around 0 V *vs* Ag|AgCl, KCl_{sat}) of the working electrode is considered as useful for selectivity of electrochemical sensor to H₂O₂, whereas at higher potentials probability of interfering oxidation reactions of other electrochemically active species that might be present in the analysed sample increases [10,40].

Considering that PB is likely the best electrochemical transducer for H₂O₂ reduction reaction, it is reasonable that PB is widely used in formation of enzymatic biosensors which use glucose oxidase (GOx) [10,36,40] or some other hydrogen peroxide-producing enzymes [27,41] as biological recognition elements. Electrochemical biosensors developed by combining PB with GOx seem to be highly advantageous for detection of glucose, which is a substrate of GOx, whereas glucose biosensors of this composition usually exhibit high selectivity, wide detection range, and they do not require the usage of soluble redox mediators [19,42,43]. Moreover, PB combined with GOx potentially could be also used for electrochemical detection of GOx inhibitors, e.g., highly toxic Hg²⁺ ions. Combination of PB with GOx for developing an amperometric Hg²⁺ ion biosensor seems to be very promising, since such biosensor could operate at relatively low potential (~ 0 V *vs* Ag|AgCl, KCl_{sat}) [10], increasing the reliability of Hg²⁺ concentration measurement. For a sake of comparison, earlier developed amperometric GOx inhibition-based Hg²⁺ ion biosensors operated at relatively high potentials from +0.4 V to +0.7 V *vs* Ag|AgCl, KCl_{sat} [44-47]. At such potentials (from +0.4 V to +0.7 V *vs* Ag|AgCl, KCl_{sat}) oxidation of other substances (e.g., alkylphenols, sulphite ion), which might be present in a sample of water or sediments, can occur [48-50], making Hg²⁺ ion analysis less reliable.

1.2.2. Dependence of the electrochemical properties of PB and PBSA on the pH value and the concentration of reduction-promoting ions

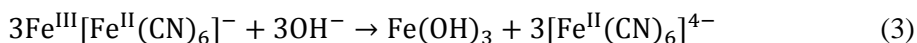
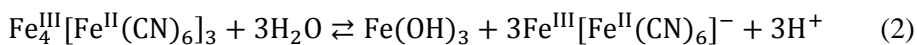
When PB (or PBSA) is electrochemically reduced, insertion of certain ions into the crystal lattice is usually necessary to ensure the charge neutrality of newly-formed reduced compound [2,51]. Reduction potential of PB and PBSA (e.g., NiHCF, CoHCF) depends on type and concentration of these ions, enabling PB and PBSA to be used in voltammetry-based detection of Li⁺, Na⁺, K⁺, Rb⁺ and other ions [51]. Furthermore, considering that PB and PBSA are electrochromic materials, dependency of PB and PBSA reduction potential on reduction-promoting ions concentration could be applied in development of electrochromic sensors and biosensors. More particularly, if the constant potential is applied to the PB (or PBSA)-coated electrode, PB and

PBSA could be possibly used as electrochromic sensors for Li^+ , Na^+ , K^+ , NH_4^+ , etc. ions. In addition, combining PB (or PBSA) with ions-producing enzymes (e.g., urease) could enable to form electrochromic biosensors for certain compounds (e.g., urea). Development of electrochromic sensors and biosensors, especially self-powered ones, seems to be promising as these sensors can help to simplify instrumentation and to save energy required for analysis [52].

H^+ ion plays an important role in charge transfer mechanism through the PB films. Studies conducted by J. J. Garcia-Jereno et al. [53,54] suggested that H^+ ions participate in an electron-hopping conduction mechanism through the PB films, whereas increment in H^+ concentration results in increased value of PB reduction current without significantly changing reduction potential of PB [53]. Moreover, electrochemical impedance spectroscopy investigation indicated that increased concentration of H^+ results in decreased value of charge transfer resistance through the PB film [54], further highlighting the importance of H^+ in transferring charge through the PB layer. This characteristic of PB – the dependency of charge transfer resistance through the PB layer on pH – have been successfully applied in developing PB-based impedimetric biosensor for urea [55]. However, additional investigation should be performed in order to clarify the role of H^+ ions in a charge conductance through the other PBSA films.

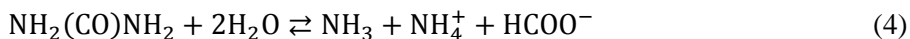
1.2.3. Dependence of PB optical properties on pH

Studies by R. Koncki et al. [24,56,57] indicated that the “insoluble” form of PB exhibits pH-dependant optical properties. It was found that an increase in pH of solution causes reversible hydrolysis of PB (Eq. 2) that results in bleaching of PB coating. This reversible hydrolysis of PB can be observed in pH range from 3 to 8-9 [24,56,57]. However, at $\text{pH} > 9$ irreversible hydrolysis resulting in degradation of PB (Eq. 3) occurs. Therefore, coatings of “insoluble” PB are suitable for optical detection of pH changes in pH interval from 3 to 8-9.



Considering that some enzymatic reactions cause changes in pH of the solution, PB can be applied in biosensing due to its optical sensitivity on pH. Therefore, “insoluble” PB has been successfully applied in construction

of optical biosensors for urea [24,57] operating due to local pH increment caused by urease-catalysed hydrolysis of urea (Eq. 4). Even though earlier developed [24] “insoluble” PB-based biosensor exhibited appropriate linear range from 2 mM to 12 mM that covers normal urea concentration in blood (up to 7.5 mM [58]), PB hydrolysis-based biosensors have several drawbacks: (i) their sensitivity depends on the buffer capacity of the sample [24], (ii) too high (≥ 9) local increment in pH might result in irreversible hydrolysis of “insoluble” PB [24,56,57]. Nevertheless, until this research an impact of pH on optical properties of “soluble” PB has not been investigated.



Taking into account previously mentioned drawbacks of applying optical PB sensitivity to pH in biosensorics and high importance [58] of monitoring urea concentration in the blood and other samples, it would be convenient to find alternative way of applying PB in urea biosensing. One of the solutions would be to develop a urea biosensor based on the electrochromic properties of PB, since the potential of the electrochromic transition between PB and PW seems to be almost independent of pH [53,54].

2. EXPERIMENTAL

2.1. Materials

$\text{FeCl}_3 \cdot 6\text{H}_2\text{O}$, $\text{CoCl}_2 \cdot 6\text{H}_2\text{O}$, $\text{K}_3[\text{Fe}(\text{CN})_6]$, NH_4Cl , K_2HPO_4 , NaH_2PO_4 , NaOH , and KOH of “highest purity”, HCl (35 %), acetone ($\geq 99.8\%$), urea ($\geq 99.5\%$), D (+)- glucose (p. ACS), enzymes glucose oxidase (approx. 280 U/mg material) and urease (≥ 220 U/mg material) were purchased from ROTH (Karlsruhe, Germany). HgCl_2 ($\geq 95\%$) acquired from VWR (Radnor, USA). Ethylenediaminetetraacetic acid disodium salt dihydrate (EDTA) (99.0% – 101.0%), fluorine doped tin oxide coated glass slides (glass|FTO) with of 2 mm thickness, indium tin oxide coated glass slide (glass|ITO) of 1 mm thickness, hydrogen peroxide (50% in water), MICRO®-90 concentrated cleaning solution and glutaraldehyde 25% solution in H_2O were purchased from SIGMA-ALDRICH (Munich, Germany). Ultra-pure water ($R \geq 18 \text{ M}\Omega$) cleaned by Milli Q-plus- Millipore system (Burlington, USA) was used to prepare solutions.

2.2. Equipment for electrochemical and optical investigations

Electrochemical investigations were performed in a three-electrodes mode using a $\mu\text{AUTOLAB}$ potentiostat/galvanostat from ECO-Chemie (Utrecht, The Netherlands). Pt wire used as a counter electrode; $\text{Ag}|\text{AgCl}$, KCl_{sat} electrode – as a reference electrode; glass|ITO or glass|FTO – as a working electrode.

USB4000 spectrometer from Ocean Optics (Largo, USA) and Perkin Elmer Lambda 25 UV|VIS spectrometer (Waltham, USA) were used for optical absorption measurements.

Hitachi TM3000 SEM coupled with X-ray energy dispersion spectrometer used for X-ray diffraction (XRD) and X-ray energy dispersion spectrometry (EDS) investigations.

2.3. Deposition of PB and CoHCF layers

Electrodes (glass|ITO or glass|FTO) were modified with PB or CoHCF layer by applying electrochemical procedures based on earlier studies [40,59,60,61].

Before modifying electrodes (glass|ITO or glass|FTO) with PB (or CoHCF) layer, electrodes were cleaned by applying ultrasound treatment (i)

in a 2% laboratory dish cleaning solution of “micro 90”, (ii) in acetone, (iii) in ultrapure water for 8-16 min during each step of the treatment (i, ii and iii).

PB was deposited electrochemically from the solution consisted of 1 mM of $\text{FeCl}_3 \cdot 6\text{H}_2\text{O}$ and 1 mM of $\text{K}_3[\text{Fe}(\text{CN})_6]$. In a case of developing biosensors for Hg^{2+} ions and urea, 0.1 M of HCl was also added into the deposition solution to improve the quality of electrochemically-formed PB [10,36]. Electrochemical deposition of PB was carried out by applying potential cycling [40,59] in the potential range between +0.4 V and +0.8 V (vs $\text{Ag}|\text{AgCl}$, KCl_{sat}) at a scan rate of 40.0 mV s^{-1} . 40 voltammetric cycles were applied. Taking into account considerations [62] that after synthesizing PB it should be presented in “insoluble” form, PB-coated electrodes (glass|ITO|PB or glass|FTO|PB) were treated by cyclic voltammetry in 0.1 M KCl solution to electrochemically stabilise PB layer by converting it into “soluble” PB form [17,62]. Considering stabilising effect of acidic media on crystalline structure of PB [10,36], 0.1 M of HCl was additionally added into KCl (0.1 M) solution when PB was electrochemically stabilised during development of Hg^{2+} ion and urea biosensors. Electrochemical stabilisation of PB was performed by applying 20 voltammetric potential scans from $0 \pm 0.05 \text{ V}$ to $+0.45 \pm 0.05 \text{ V}$ (vs $\text{Ag}|\text{AgCl}$, KCl_{sat}) at a scan rate of 40.0 mV s^{-1} . The glass|ITO|PB electrode containing electrochemically stabilised PB layer was used as an electrochromic ammonium ion sensor.

A layer of CoHCF was deposited on the glass|ITO electrode by adjusting cyclic voltammetry-based procedures from previous studies [60,61]. The electroplating bath solution consisted of $\text{CoCl}_2 \cdot 6\text{H}_2\text{O}$ (1 mM), $\text{K}_3[\text{Fe}(\text{CN})_6]$ (1 mM) and KCl (500 mM) was prepared by mixing two distinct solutions ((a) and (b)): (a) 45 mL of $\text{K}_3[\text{Fe}(\text{CN})_6]$ (1.11 mM) and KCl (556 mM); (b) 5 mL of $\text{CoCl}_2 \cdot 6\text{H}_2\text{O}$ (16.7 mM). In order to avoid the spontaneous precipitation of CoHCF [61], both (a) and (b) solutions were deoxygenized by purging solutions with nitrogen gas before mixing together. A layer of CoHCF was deposited on the glass|ITO electrode (glass|ITO|CoHCF) from freshly prepared electroplating bath solution by applying potential cycling from +0.1 V to +0.9 V (vs $\text{Ag}|\text{AgCl}$, KCl_{sat}) at the scan rate of 50.0 mV s^{-1} . 60 potential cycles were applied. In order to obtain the oxidised state of CoHCF layer (glass|ITO|CoHCF_{ox} electrode), the potential scanning during CoHCF deposition was ended at +0.9 V vs $\text{Ag}|\text{AgCl}|\text{KCl}_{\text{sat}}$, since at this potential CoHCF is presented in oxidised state (CoHCF_{ox}) [7,61,63]. Taking into account that redox cycling of PB in K^+ ions-containing solution helps to improve electrochemical properties of PB [17,62], in this research the glass|ITO|CoHCF electrode was treated by potential cycling in K^+ ions-

containing solution as well. Briefly – the glass|ITO|CoHCF electrode was treated by potential cycling (15 voltammetric cycles) from +0.9 V to +0.1 V (vs Ag|AgCl, KCl_{sat}) in the 0.5 M KCl solution at the scan rate of 50.0 mV s⁻¹; the potential sweep was terminated at +0.9 V (vs Ag|AgCl, KCl_{sat}). After this procedure obtained glass|ITO|CoHCF_{ox}|KCl_{cycled} electrode was used as an optical hydrogen peroxide sensor. An impact of glass|ITO|CoHCF electrode treatment by cycling it in 0.5 M KCl solution on chemical composition of CoHCF layer was investigated by EDS method.

2.4. Immobilisation of enzymes on a PB layer

In order to construct biosensors for urea and Hg²⁺ ion, enzymes urease and glucose oxidase (GOx) were immobilised on electrochemically stabilised PB layers. Urease was immobilised on the glass|ITO|PB electrode, obtaining glass|ITO|PB|urease biosensor for urea, while GOx was immobilised on the glass|FTO|PB electrode, forming the glass|FTO|PB|GOx-based biosensor for Hg²⁺ ions. Immobilisation of urease on the glass|ITO|PB electrode was performed by dispersing 7 µL of urease solution (20 mg mL⁻¹) on the PB layer of the glass|ITO|PB electrode (0.7 cm² geometric area), drying the electrode at room conditions and then incubating the urease-covered electrode above the solution of glutaraldehyde (25 %) for 15 min to cross-link the enzyme [64]. Similar procedure was used to immobilise GOx on the PB layer of the glass|FTO|PB electrode, briefly: 15 µL of 15 mg mL⁻¹ GOx solution was dispersed on the surface of PB layer (1 cm²) and then left to dry at room conditions; the immobilisation of GOx was completed with incubation above the glutaraldehyde solution (25 %) for 15 min.

2.5. Investigation of the electrochromic ammonium ion sensor (glass|ITO|PB electrode)

The electrochromic ammonium ion sensor (glass|ITO|PB) was investigated in an optically-transparent glass cuvette filled with aqueous NH₄Cl solutions of various concentrations (from 0.01M up to 0.1 M). Potential of +0.2 V (vs Ag|AgCl, KCl_{sat}) was applied to the glass|ITO|PB electrode while recording absorption spectrum.

2.6. Investigation of the electrochromic urea biosensor (glass|ITO|PB|urease)

The electrochromic glass|ITO|PB|urease biosensor was investigated in an optically-transparent glass cuvette filled with urea-containing PBS, pH 5.5. K^+ ions-free, Na^+ ions-containing PBS prepared by dissolving NaH_2PO_4 (0.01 M) and NaOH (0.1 M) into ultra-pure water was chosen for investigations of urea biosensor, since Na^+ ions are not considered to promote PB conversion into PW [10,12]. Absorption spectra of the glass|ITO|PB|urease biosensor were recorded 2 min after the addition of urea into PBS under conditions of a constant +0.2 V (vs Ag|AgCl, KCl_{sat}) potential. Between investigations in PBS (pH 5.5) containing different concentration of urea, the biosensor was regenerating by immersing it into PBS (pH 5.5) for 1 min.

Taking into account that urease-catalysed hydrolysis of urea results in increase in pH that might influence optical properties of PB [24,56,57], in this research the glass|ITO|PB|urease biosensor was investigated in PBS of different pH (from 5.5 to 12). During this research the glass|ITO|PB|urease biosensor was immersed in PBS with certain pH value for 2 min before registering absorption spectrum. To maintain control conditions, during this experiment potential of +0.2 V (vs Ag|AgCl, KCl_{sat}) was applied to the glass|ITO|PB|urease biosensor. Between investigations in PBS with different pH value, the biosensor was regenerated by immersing it into PBS (pH 5.5) for 1 min.

2.7. Investigation of CoHCF-based optical H_2O_2 sensor (glass|ITO|CoHCF_{ox}| KCl_{cycled} electrode)

The optical H_2O_2 sensor (glass|ITO|CoHCF_{ox}| KCl_{cycled} electrode) was investigated in an optically-transparent glass cuvette filled with 0.5 M KCl solution containing different concentrations of H_2O_2 (from 1.5 mM to 20 mM). Absorption spectra of the glass|ITO|CoHCF_{ox}| KCl_{cycled} electrode were registered 5 min after immersing the sensor into 0.5 M KCl solution containing certain concentration of H_2O_2 . After investigating the glass|ITO|CoHCF_{ox}| KCl_{cycled} electrode in H_2O_2 -containing KCl solution, the electrode was re-oxidised by applying cyclic voltammetry in the 0.5 M KCl solution - 15 voltammetric cycles from +0.9 V to +0.1 V (vs Ag|AgCl, KCl_{sat}) (scan rate 50.0 mVs^{-1}) were applied to the glass|ITO|CoHCF_{ox}| KCl_{cycled} electrode.

Hitachi TM3000 SEM coupled with X-ray energy dispersion spectrometer used for X-ray diffraction (XRD) and X-ray energy dispersion spectrometry (EDS) investigations of Cobalt hexacyanoferrate films. EDS spectra were recorded at accelerating voltage of 5 kV and accumulation time of 5 min. $\theta/2\theta$ and grazing incidence X-ray diffraction (XRD and GI-XRD) patterns were collected by using a Bruker D8 Advance diffractometer with Cu K α radiation ($\lambda=0.15406$ nm). GI-XRD measurements were obtained using incident X-ray beam angle of 1° . The diffraction patterns were analysed using Topas (Bruker AXS) software (version 4.2) following the Le Bail decomposition procedure and Rietveld refinement.

2.8. Investigation of the amperometric Hg^{2+} ion biosensor (glass|FTO|PB|GOx)

The glass|FTO|PB|GOx biosensor was investigated amperometrically in PBS (pH 7) at a constant potential of +0.2 V (vs Ag|AgCl, KCl_{sat}) by adding a constant amount of glucose (1.3 mM) and various concentrations of HgCl_2 (27 μM to 247 μM) into PBS. The working principle of this biosensor (glass|FTO|PB|GOx) is based on measuring Hg^{2+} ion-caused changes in reduction current of H_2O_2 which is a product of GOx-catalysed glucose oxidation reaction. The Hg^{2+} -caused decrement in H_2O_2 reduction current (dj , %) was evaluated by using equation (5) [47]:

$$dj = \frac{I_0 - I_i}{I_0} \cdot 100\% \quad (5)$$

where I_0 is the reduction current measured after addition of glucose into PBS and I_i is the reduction current measured after addition of glucose and analyte (Hg^{2+} ions) that acted as inhibitor into the electrochemical cell.

3. RESULTS AND DISCUSSION

3.1. Investigation of the electrochromic ammonium ion sensor (glass|ITO|PB electrode)

3.1.1. Electrochemical stabilisation of a PB layer

Taking into account considerations [62] that after PB synthesis it should be presented in “insoluble” form, the glass|ITO|PB electrode was treated by cyclic voltammetry in 0.1 M KCl solution to electrochemically stabilise [17,62] PB layer by converting it into “soluble” PB form (Fig. 1A) [65]. The shape of redox peaks in cyclic voltammograms became narrower while applying the first six potential scans and did not change during further potential cycling (Fig. 1A), indicating transition of “insoluble” PB into “soluble” form [3,17]. Moreover, some changes in absorption spectrum of the glass|ITO|PB electrode have been observed after applying potential cycling in KCl solution – maximum of the glass|ITO|PB electrode absorption increased from 0.418 u.a. (before stabilization) to 0.449 u.a. (after stabilization) and the wavelength of absorption maximum shifted from 720 to 707 nm (Fig. 1B). These effects - an increase in absorption and shift of absorption maximum to lower wavelengths observed after transforming PB from the “insoluble” to the “soluble” form – have been reported in earlier studies as well [24,66]. In the research performed by R. Koncki et al. [24] a shift of wavelength corresponding absorption maximum from 720 nm to 708 nm was observed, while Mortimer and Rosseinsk [66] obtained wavelength shift from 730 nm to 690 nm. Therefore, it can be concluded that the PB layer of the glass|ITO|PB electrode was successfully transformed into electrochemically more stable “soluble” form after applying cyclic voltammetry in 0.1 M KCl solution.

The half-wave potential of PB calculated from the voltammograms in Fig. 1A was +0.18 V (*vs* Ag|AgCl, KCl_{sat}). By making a presumption that NH₄⁺ ion-caused changes in redox state of PB should be optically observed when potential applied to the glass|ITO|PB electrode is close to PB reduction potential, potential value of +0.2 V (*vs* Ag|AgCl, KCl_{sat}), which is very close to +0.18 V, was chosen for investigation of the glass|ITO|PB electrode in ammonium ion-containing solution.

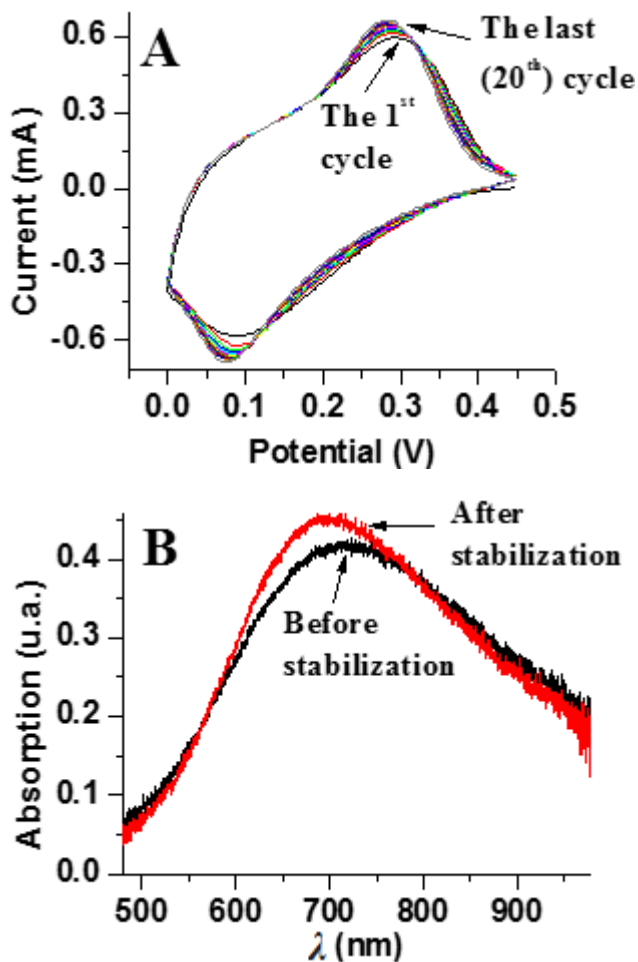


Fig. 1. **A** – cyclic voltammograms of the glass|ITO|PB electrode recorded in 0.1M KCl solution during electrochemical stabilization of the PB layer. **B** – absorption spectra of the glass|ITO|PB electrode measured in 0.1 M KCl solution before and after the stabilization procedure.

3.1.2. Investigation of the electrochromic response of the glass|ITO|PB electrode to ammonium ions

Investigation of the glass glass|ITO|PB electrode in NH_4^+ solutions of various concentrations (from 0.01M to 0.1 M) indicated that the position and value of the glass|ITO|PB sensor absorption maximum are dependent on NH_4^+ ions concentration in the solution (Fig. 2A). The intake of NH_4^+ ions in the electrochemical cell caused the decrease in the intensity of maximal absorption and shifting of λ_{max} to longer waves. By plotting the absorption at

a given wavelength of 730 nm (Fig. 2B) and/or λ_{max} against the concentration of ammonium ions (Fig. 2C), the linear dependencies curves were registered in both cases. The glass|ITO|PB sensor appeared to be suitable for detecting ammonium ions concentration in the range from 0.01 M to 0.10 M.

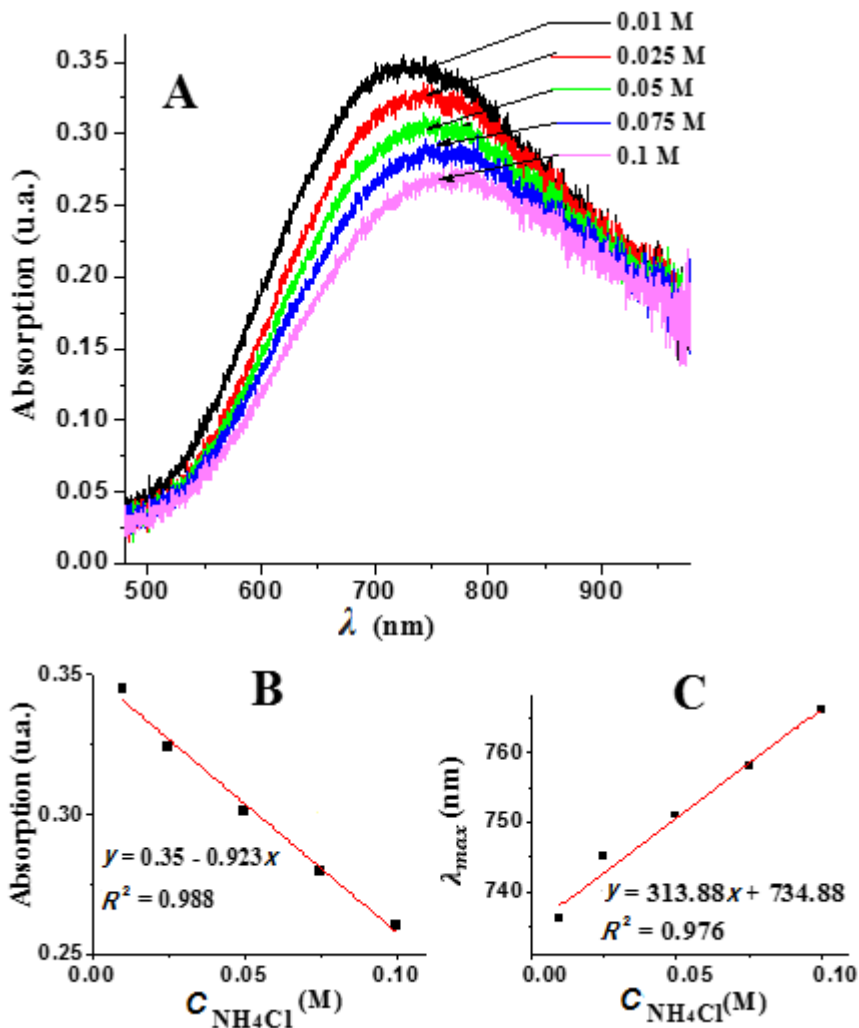
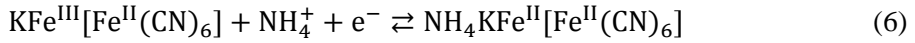


Fig. 2. **A** – absorption spectra of the glass|ITO|PB sensor registered in NH_4Cl solutions of various concentrations (from 0.01 M to 0.10 M). Absorption spectra were registered while applying +0.2 V potential to the sensor. **B** – plot of absorption vs concentration of ammonium ions at a wavelength of 730 nm. **C** – plot of wavelength of absorption maximum vs concentration of ammonium ions.

The NH_4^+ ions-caused decrement in absorption of PB layer of the glass|ITO|PB electrode (Fig. 2) should be related to transition of deep blue-colored PB into transparent PW. During the electrochemical reduction of PB, some cations (e.g., K^+ and NH_4^+) are intercalated to the crystal lattice of PB to compensate the charge [2,10,36]. An example of charge compensation by intercalation of NH_4^+ ion into “soluble” PB is given in Eq. 6 [11]. Furthermore, it is considered [51] that reduction potential of PB depends on the type and concentration of PB reduction-promoting cations. According to the research performed by Dussel et al. [51], PB reduction reaction in NH_4^+ ions-containing solution can be divided into two equilibria: equilibrium between oxidised and reduced states of iron ion (Eq. 7) and equilibrium between free and intercalated NH_4^+ ions (Eq. 8)



Characterizing activities (a) of oxidised and reduced species such as $a(\text{Fe}^{3+})$ and $a(\text{Fe}^{2+} \text{NH}_4^+)$, respectively, the potential of PB reduction reaction can be expressed by Nernst equation [51] modified in a following way:

$$E = E^0 - \frac{RT}{nF} \ln K + \frac{RT}{nF} \ln \frac{a(\text{Fe}^{3+})}{a(\text{Fe}^{2+} \text{NH}_4^+)} + \frac{RT}{nF} \ln a(\text{NH}_4^+) \quad (9)$$

where E^0 is a standard potential of Prussian blue reduction reaction, R is universal gas constant, T is temperature (in Kelvin), F is Faraday constant and K is equilibrium constant derived from (8) equation:

$$K = \frac{a(\text{Fe}^{2+})a(\text{NH}_4^+)}{a(\text{Fe}^{2+} \text{NH}_4^+)} \quad (10)$$

Addition of ammonium ions to electrochemical cell causes the increase in PB reduction potential (Eq. 9). Thus, if the constant value of electric potential (+0.2 V vs Ag|AgCl, KCl_{sat}) is applied to the glass|ITO|PB sensor, increment in ammonium ions concentration should result in electrochemical reduction of some PB units into PW form (Eq. 6), causing decrement in PB absorption (Fig. 2). Therefore, it can be concluded that NH_4^+

ion-caused decrement in PB absorption (Fig. 2) is related to transition of PB into PW form.

3.2. Investigation of the electrochromic urea biosensor (glass|ITO|PB|urease)

3.2.1. Investigation of the glass|ITO|PB|urease biosensor in urea-containing PBS

Urease is often involved in composition of urea biosensors, since the enzymatic hydrolysis of urea (Eq. 4) is accompanied with the variation of many measurable characteristics, e.g., increment in CO_2 and NH_4^+ concentrations [67], changes in temperature and pH [67,68]. Considering previously obtained results indicating that optical absorption of PB depends on NH_4^+ ions concentration when +0.2 V vs Ag|AgCl, KCl_{sat} potential is applied to the PB-coated electrode (glass|ITO|PB) (Fig. 2), it was decided to develop the electrochromic urea biosensor by immobilising an enzyme urease on the glass|ITO|PB electrode (glass|ITO|PB|urease) [69]. The electrochromic glass|ITO|PB|urease biosensor was investigated under the similar condition as previously investigated ammonium ion sensor (Fig. 2) – a constant potential of + 0.2 V (vs Ag|AgCl, KCl_{sat}) was applied to the working electrode during its investigation in urea-containing PBS. The scheme representing operation of the glass|ITO|PB|urease biosensor is given in Fig. 3. An addition of urea into PBS caused the fading of PB layer of the glass|ITO|PB|urease biosensor that is considered to be caused by reduction of PB into PW. After investigating the glass|ITO|PB|urease biosensor in urea-containing PBS, the biosensor was regenerated by simply immersing it in PBS (pH 5.5) solution for 1 min (Fig. 3) to re-oxidise PW to PB.

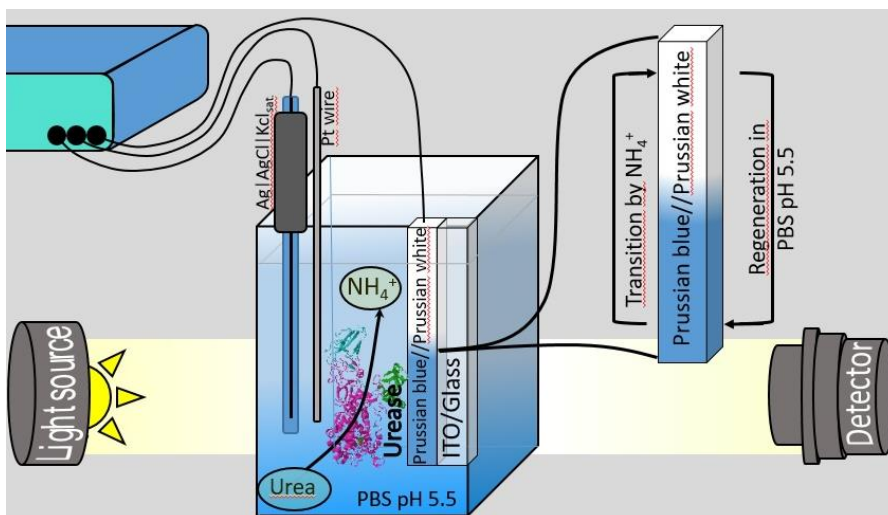


Fig. 3. The scheme representing operation of the glass|ITO|PB|urease biosensor.

Absorption spectra measured during investigation of the glass|ITO|PB|urease biosensor in urea-containing PBS are given in Fig. 4. As it is seen from the data presented in Figure 4, the value of optical absorption maximum of the glass|ITO|PB|urease biosensor decreased with higher concentration of urea in PBS. In order to relate the intensity of the glass|ITO|PB|urease biosensor's absorption with concentration of urea, the difference in maximal absorption (ΔA) was calculated by subtracting maximal absorption measured in urea-containing PBS from maximal absorption measured in pure PBS (data from Fig. 4). The linear dependency between urea concentration and ΔA was obtained in concentration range from 3 mM to 30 mM of urea with sensitivity of approx. 4.2 u.a. mM⁻¹ (Fig. 5). The linear range obtained during the investigation of the glass|ITO|PB|urease (from 3 mM to 30 mM) was wider than linear range (from 2 mM to 12 mM) obtained during previous investigation of the urease biosensor based on pH-induced changes in absorption of "insoluble" PB [24]. Nevertheless, both linear ranges (from 3 mM to 30 mM and from 2 mM to 12 mM) covers normal urea concentration in blood (up to 7.5 mM [58]).

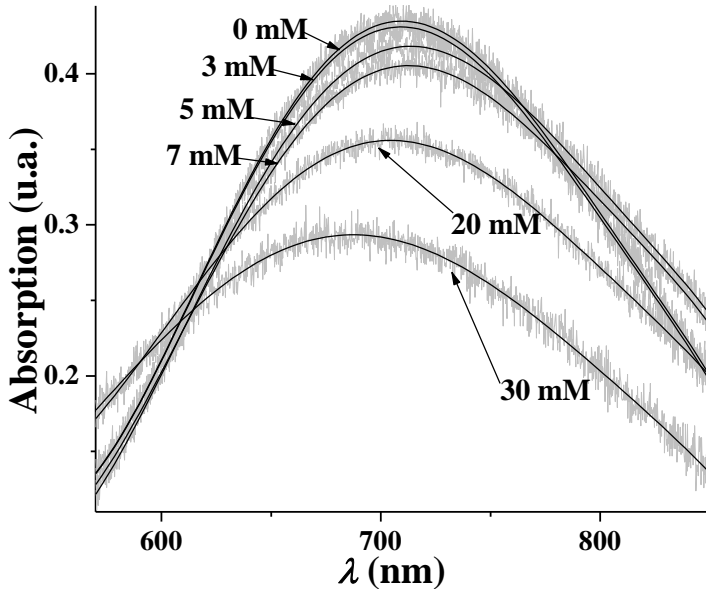


Fig. 4. Investigation of the glass|ITO|PB|urease biosensor in urea-containing PBS. Absorption spectra were recorded 2 min after the addition of urea into PBS. During investigation a constant potential of +0.2 V (vs Ag|AgCl, KCl_{sat}) was applied to the biosensor.

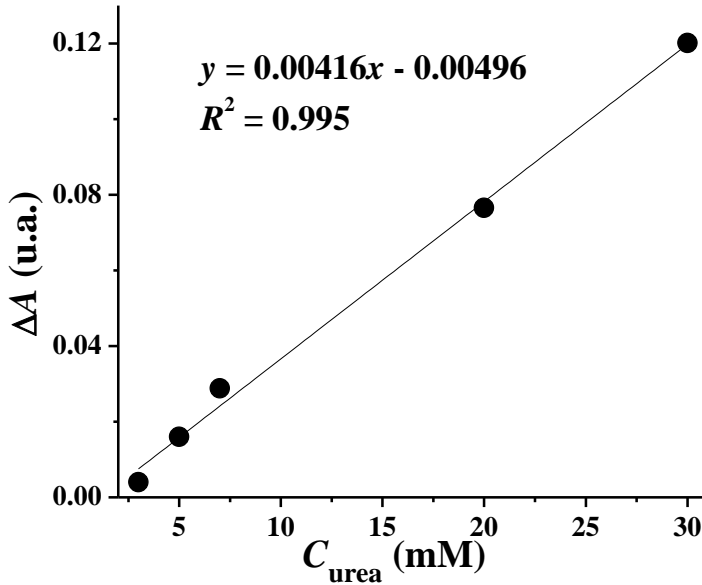


Fig. 5. Linear dependence of urea-caused change in absorption (ΔA) on urea concentration in PBS.

After investigating the glass|ITO|PB|urease biosensor in each concentration of urea, the biosensor was regenerated by immersing it into PBS (pH 5.5) for 1 min. Absorption spectrum, recorded before the investigation of glass|ITO|PB|urease biosensor in urea solution, and absorption spectrum, recorded after the regeneration, had the same form (Fig. 6), making this biosensor suitable for repeated analysis of urea. The process of the glass|ITO|PB|urease biosensor regeneration in PBS (pH 5.5) could be explained by spontaneous oxidation of PW into PB: during investigation of the glass|ITO|PB|urease biosensor in urea solution, the presence of enzymatically-generated NH_4^+ ions and the application of reductive potential (+0.2 V) caused electrochromic transition of PB into PW form, observed as a decrease in PB absorption spectrum (Fig. 6, curve 2 and 4). However, PW has a tendency to re-oxidise into PB due to the impact of oxygen in solution, thus, the absence of reduction potential (+0.2 V vs Ag|AgCl|KCl sat) and NH_4^+ ions leads to spontaneous oxidation of PW into PB [31,33,34].

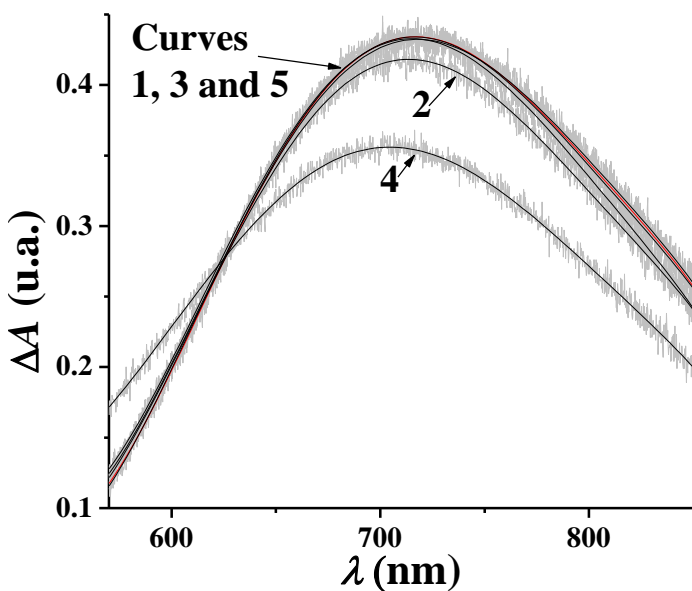


Fig. 6. Absorption spectra recorded using glass|ITO|PB|urease biosensor. Curve 1 – before the addition of urea into PBS. Curve 2 – 2 min after the addition of 5 mM of urea in PBS. Curve 3 – after the regeneration of glass|ITO|PB|urease biosensor by immersing it into PBS. Curve 4 – 2 min after the addition of 20 mM of urea in PBS. Curve 5 – after the second regeneration of glass|ITO|PB|urease biosensor. Absorption spectra 1, 3 and 5 having the same form were measured in PBS without urea added.

In order to evaluate the stability of the glass|ITO|PB|urease biosensor response to urea over time, the glass|ITO|PB|urease biosensor was investigated in PBS containing 30 mM urea repeatedly during a time period of 41 days. Stability of the biosensor response to urea was calculated by dividing ΔA value measured 10, 21 and 41 days after manufacturing the glass|ITO|PB|urease biosensor ($\Delta A_{\text{repeated}}$) by the value of ΔA measured during the day of manufacturing the biosensor ($\Delta A_{\text{initial}}$), i. e. stability of biosensor response = $\Delta A_{\text{repeated}}/\Delta A_{\text{initial}}$ (Table 1). In comparison to the initial response of the glass|ITO|PB|urease biosensor response to urea (100%), stability of the biosensor response to urea remained greater than 50 % during the time period of 41 days.

Table 1. Stability of the glass|ITO|PB|urease biosensor response to 30 mM urea concentration measured during the time period of 41 days.

Days after manufacturing the glass ITO PB urease biosensor	Stability of the biosensor response, %
10	83
21	55
41	51

3.2.2. Evaluation of the pH influence on the optical properties of the glass|ITO|PB|urease biosensor

Earlier studies [24,56,57] indicated that the intensity of “insoluble” PB optical absorption depends on pH. The increase in pH, occurring due to urease catalysed hydrolysis of urea, causes the decrease in PB absorption [24,56,57]. The same effect – the decrease in PB absorption – has been observed when PB-coated electrode (glass|ITO|PB) was investigated in ammonium ion-containing solution under conditions of +0.2 V (*vs* Ag|AgCl, KCl_{sat}) potential applied to the glass|ITO|PB electrode (Fig. 2). Therefore, to clarify the origin of the glass|ITO|PB|urease biosensor sensitivity to urea, in this research the influence of pH on the absorption spectrum of the glass|ITO|PB|urease biosensor was evaluated as well.

It was determined that initial pH (5.5) of PBS containing 30 mM of urea did not change after 2 min lasting investigation of the biosensor. This finding shows proper buffering capacity of selected PBS. However, it can be presumed that during investigation of the glass|ITO|PB|urease biosensor in urea-containing PBS, the local pH changes near to the electrochromic PB layer are greater than the pH change in bulk solution, thus local changes of pH might

be high enough to generate significant decrease in optical absorption of PB. In order to evaluate the impact of alkaline pH on PB absorption, the glass|ITO|PB|urease biosensor was investigated in PBS with pH values varying from 5.5 to 12. After 2 min lasting glass|ITO|PB|urease biosensor immersion in PBS with pH value ranging from 5.5 to 11, the absorption spectrum of the glass|ITO|PB|urease biosensor has not changed (Fig. 7). On the contrary, 2 min lasting measurement of glass|ITO|PB|urease biosensor in PBS at pH 12 caused the exfoliation of PB|urease layer from the surface of the glass|ITO|PB|urease biosensor [data not presented].

It can be presumed that during the 2 min-lasting investigation of glass|ITO|PB|urease biosensor in PBS with pH ranging from 5.5 to 11, reversible hydrolysis of PB, which has been reported for “insoluble” PB coatings [24,56,57], has not occurred or could not be observed due to the slow rate of hydrolysis reaction. The inertness of the glass|ITO|PB|urease sensor to pH (in range the from 5.5 to 11) might be related to the usage of “soluble” PB in composition of the glass|ITO|PB|urease. As far as is known, only “insoluble” form of PB has been reported to be optically sensitive to the changes in pH of solution [24,56,57]. Furthermore, taking into account the effective regeneration of the glass|ITO|PB|urease biosensor after investigating it in urea-containing PBS (Fig. 6), the irreversible exfoliation of PB layer, which occurred at pH 12, should not be considered as suitable explanation for the operation of glass|ITO|PB|urease biosensor, since the layer of PB cannot be regenerated after exfoliation. Summarising these results, it can be concluded that the ammonium-caused electrochromic transition of PB into PW under conditions of +0.2 V (*vs* Ag|AgCl, KCl_{sat}) potential applied to the working electrode (Fig. 4) seems to be the only explanation of the glass|ITO|PB|urease biosensor sensitivity to urea. Furthermore, the insensitivity of the glass|ITO|PB|urease biosensor to pH should enable to overcome a common problem of optical “insoluble” PB-based urea biosensors – dependency of biosensor sensitivity on buffer capacity of the sample [24].

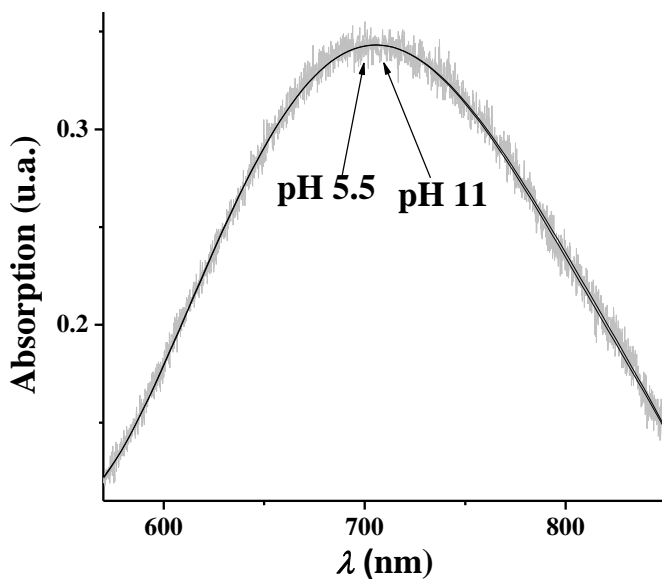
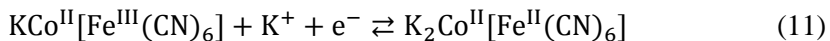


Fig. 7. Investigation of the glass|ITO|PB|urease biosensor in PBS of various pH. No pH-induced change in absorption spectrum of the glass|ITO|PB|urease biosensor was observed in a pH range from 5.5 to 11. At pH 12 the PB|urease layer has exfoliated from the glass|ITO electrode.

3.3. Investigation of CoHCF-based optical sensor for hydrogen peroxide

3.3.1. Investigation of electrochemical and electrochromic properties of CoHCF

CoHCF can exist in two different forms: (i) inserted cation-containing form, $XCo[Fe(CN)_6]$, where X is alkali metal cation inserted in the crystal lattice of CoHCF and (ii) inserted cation-free form ($Co_2[Fe(CN)_6]$) [7]. To achieve a sufficient electrochromic performance of CoHCF, it should be presented in inserted cation-containing form, since the inserted cation-free form of CoHCF ($Co_2[Fe(CN)_6]$) is considered to be almost electrochemically inactive [7]. When CoHCF is synthesized in inserted cation-containing form, the “ideal” stoichiometric ratio of X^+ , Co^{2+} and Fe^{3+} ions is 1:1:1, however, this ratio (1:1:1) could be changed due to the formation of defect sites where Co^{2+} ion is not fully coordinated to the $[Fe(CN)_6]^{4-}$ ligands [61,63]. Furthermore, electrochromic transition between oxidised and reduced states of inserted cation-containing CoHCF appears due to reduction and oxidation of Fe^{2+}/Fe^{3+} ions [63]. The general oxidation-reduction reaction of CoHCF in K^+ containing solution can be presented as follows [7]:



In order to apply CoHCF in optical sensing of hydrogen peroxide, appropriate conditions to maintain stable electrochemical CoHCF properties during multiple redox transformation and to reach the greatest difference in the absorption spectra between reduced and oxidised forms of CoHCF should be found. For this purpose, the glass|ITO|CoHCF electrode was investigated by cyclic voltammetry and absorption spectroscopy in 0.1 M and 0.5 M KCl solutions. Cyclic voltammograms of the glass|ITO|CoHCF electrode recorded in 0.5 M KCl solution exhibited a constant form and remained stable during application of 15 potential cycles from +0.9 V to +0.1 V vs Ag|AgCl, KCl_{sat} (scan rate 50 mV s^{-1}) (Fig. 8A), indicating high electrochemical stability of CoHCF layer in 0.5 M KCl solution. Moreover, it was determined [70] by energy-dispersive X-ray spectroscopy (EDS) method that chemical formula of electrochemically deposited CoHCF is $\text{K}_{1.2}\text{Co}_{1.1}[\text{Fe}(\text{CN})_6]$ and this formula ($\text{K}_{1.2}\text{Co}_{1.1}[\text{Fe}(\text{CN})_6]$) did not change after applying cyclic voltammetry (Fig. 8A) to the glass|ITO|CoHCF electrode in 0.5 M KCl solution. These findings indicate that inserted K^+ ion-containing CoHCF layer formed during electrochemical deposition of CoHCF on a glass|ITO surface maintains the constant chemical composition ($\text{K}_{1.2}\text{Co}_{1.1}[\text{Fe}(\text{CN})_6]$) and electrochemical properties after being cycled in 0.5 M KCl solution for at least 15 potential scans.

On the contrary to the results obtained in the 0.5 M KCl solution (Fig. 8A), a gradual decrement in oxidation current was observed during cyclic voltammetry investigation of the glass|ITO|CoHCF electrode in 0.1 M KCl solution (Fig. 8B). A similar decrease in electrochemical activity of CoHCF was reported in previous research as well [7] – it was suggested that potential cycling in acidic solution, which do not contain any CoHCF redox transition-promoting ions, causes restructuring of electrochemically active inserted cation-containing CoHCF into electrochemically less active inserted cation-free form. Therefore, the decrement in CoHCF oxidation current (Fig. 8B) observed during the potential cycling in 0.1 M KCl solution could be explained by transition of inserted cation (K^+)-containing CoHCF ($\text{K}_{1.2}\text{Co}_{1.1}[\text{Fe}(\text{CN})_6]$) crystal units into inserted cation-free form, caused by rather low concentration of K^+ ions in KCl solution. Furthermore, in comparison to the experiment conducted in 0.5 M KCl solution (Fig. 8A), the CoHCF layer exhibited lower oxidation and reduction peak currents even at the first potential scan in 0.1 M KCl solution (Fig. 8B). Lower peak currents observed in 0.1 M KCl could be related not only to the transformation of inserted cation-containing CoHCF

into inserted cation-free form, but also to the kinetics of CoHCF redox reactions: the rate limiting factor of CoHCF redox reactions is the diffusion of K^+ ion between CoHCF and the solution [63].

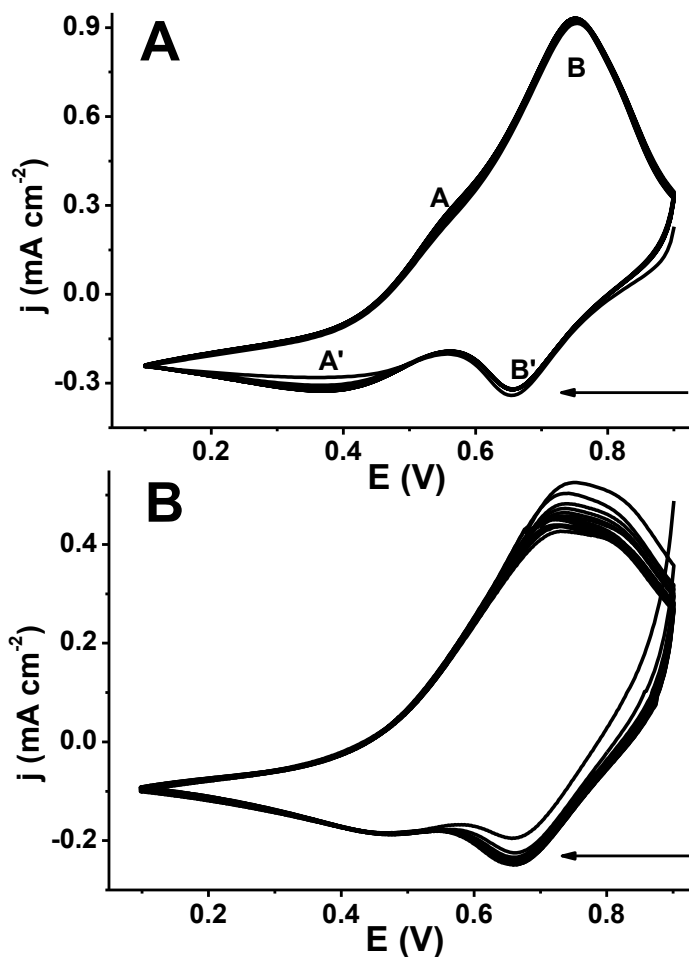


Fig. 8. **A** – cyclic voltammograms of the glass|ITO|CoHCF electrode registered in 0.5 M KCl solution. Peaks A and A' represents the oxidation/reduction reaction of Co^{2+}/Co^{3+} ions occurring due to presence of water coordinated Co^{2+}/Co^{3+} ions in CoHCF structure. Peaks B and B' indicates the redox reaction of Fe^{2+}/Fe^{3+} ions in sites of CoHCF in which Co^{2+} ions are coordinated with $[Fe(CN)_6]^{n-}$ ligands. **B** – cyclic voltammograms of the glass|ITO|CoHCF electrode registered in 0.1 M KCl solution. Scan rate 50 mV s^{-1} .

There are several explanations of two oxidation and reduction peaks observed in cyclic voltammograms of the glass|ITO|CoHCF electrode (Fig. 8A). Even though earlier research [60] suggested that double peaks of CoHCF redox reactions should be attributed to different CoHCF saturation levels with K^+ ions, a more recent investigation [63] explained the splitting of CoHCF oxidation and reduction peak currents by the presence of specific sites in the crystal lattice of CoHCF, where a part of $[Fe(CN)_6]^{n-}$ ligands is replaced by the water molecules. Taking into account that the chemical composition of CoHCF formed in this work is characterized by a 1:1.1 stoichiometric ratio between Co^{2+} and $[Fe(CN)_6]^{n-}$ ions, the presence of water-coordinated Co^{2+} ions seems to be inevitable. In these water-coordinated sites the oxidation and reduction of Co^{2+}/Co^{3+} ions occur [63] and it can be observed in cyclic voltammograms (Fig. 2A, peaks A and A'). The major peaks (Fig. 8A, peaks B and B') are attributed to oxidation/reduction of Fe^{2+}/Fe^{3+} ions in CoHCF structure.

Optical absorption spectra of the glass|ITO|CoHCF electrode at different oxidation states of CoHCF were registered correspondingly (i) in 0.5 M KCl solution after cycling in 0.5 M KCl and (ii) in 0.1 M KCl solution after cycling in 0.1 M KCl (Fig. 9A and 9B). Oxidised ($CoHCF_{ox}$) and reduced ($CoHCF_{red}$) states of CoHCF were achieved by applying +0.9 V and +0.1 V vs $Ag|AgCl, KCl_{sat}$ potential to the glass|ITO|CoHCF electrode, respectively. The difference between absorption maximum (ΔA) of the glass|ITO|CoHCF electrode in oxidised and reduced states was significantly greater in 0.5 M KCl solution ($\Delta A = 0.085$ u.a., Fig. 9A) than that in 0.1 M KCl solution ($\Delta A = 0.009$ u.a., Fig. 9B). Furthermore, absorption spectrum of CoHCF in oxidised state (Fig. 9A and 9B) exhibited a similar form in both 0.1 M KCl and 0.5 M KCl solutions, indicating that the CoHCF layer could to be partially “trapped” in oxidised state after potential cycling in 0.1 M KCl solution. A weak electrochromic transition ($\Delta A = 0.009$) of CoHCF obtained in 0.1 M KCl (Fig. 9B) corresponds to data in figure 8, indicating CoHCF transition from inserted cation-containing form into inserted cation-free form due to potential cycling in 0.1 M KCl solution. Summarising this data (Fig. 8 and 9) it can be concluded that sufficient concentration of K^+ cations (0.5 M) is required to ensure an affective redox transition between oxidised and reduced states of CoHCF. Therefore, 0.5 M concentration of KCl solution has been further applied in investigation of $CoHCF_{ox}$ optical response to hydrogen peroxide.

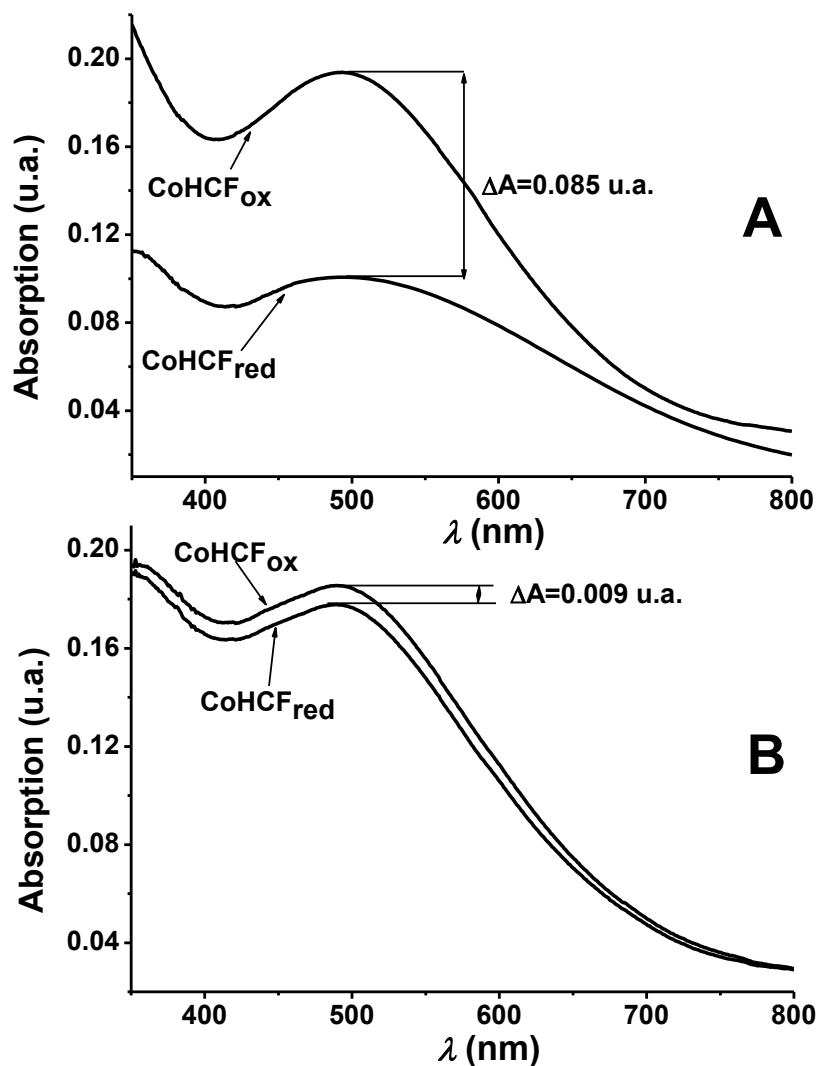


Fig. 9. Optical absorption spectra of the glass|ITO|CoHCF electrode in oxidised (CoHCF_{ox}) and reduced (CoHCF_{red}) states registered in **(A)** 0.5 M KCl solution, **(B)** 0.1 M KCl solution.

3.3.2. The impact of O₂ on the optical properties of CoHCF_{ox}

The structural analogue of CoHCF – Prussian white (PW) – can be applied in optical detection of H₂O₂ [24,31,32,34]. When transparent PW reacts with H₂O₂, it oxidises into deep-blue coloured PB. However, PW can be oxidised into PB not only due to interaction with H₂O₂, but also due to the impact of oxygen from air or solution, thus, interaction between PW and oxygen can

reduce the reliability of H_2O_2 sensing. Therefore, it is important to investigate materials which are inert towards oxygen while being optically responsive towards H_2O_2 .

In order to determine if CoHCF at oxidised state (CoHCF_{ox}) is sensitive to the impact of oxygen, the glass|ITO| CoHCF_{ox} | $\text{KCl}_{\text{cycled}}$ electrode was kept in open air within the time period of 7 days. Optical absorption spectra of the glass|ITO| CoHCF_{ox} | $\text{KCl}_{\text{cycled}}$ electrode were recorded in the spectrophotometric cell filled with ultrapure water. Optical investigations approved the predicted stability of CoHCF_{ox} layer – only minor increase of CoHCF_{ox} optical absorption spectrum was observed within the 7 days (Fig. 10A). A slight increase in CoHCF_{ox} optical absorption spectrum (Fig. 10A) should not be attributed to the change of CoHCF_{ox} oxidation state, since the decrement in absorption would be observed in a case of CoHCF_{ox} reduction (Fig. 9). Therefore, in a contrary to PW, CoHCF_{ox} layer is not supposed to lose its selectivity to hydrogen peroxide due to the impact of oxygen from air.

3.3.3. Investigation of the optical H_2O_2 sensor (glass|ITO| CoHCF_{ox} | $\text{KCl}_{\text{cycled}}$ electrode) in the hydrogen peroxide-containing solution

Optical response of the glass|ITO| CoHCF_{ox} | $\text{KCl}_{\text{cycled}}$ electrode to H_2O_2 was investigated by adding different concentrations of H_2O_2 (from 1.5 mM to 20 mM) into 0.5 M KCl solution. An example of glass|ITO| CoHCF_{ox} | $\text{KCl}_{\text{cycled}}$ electrode investigation in H_2O_2 (20 mM)-containing 0.5 M KCl solution is given in Fig. 10B. The addition of H_2O_2 into 0.5 M KCl solution caused the decrement in absorption of the CoHCF_{ox} (Fig. 10B), indicating the chemical reduction of CoHCF_{ox} . After investigating the glass|ITO| CoHCF_{ox} | $\text{KCl}_{\text{cycled}}$ electrode in KCl solution containing H_2O_2 , the layer of CoHCF was regenerated to its initial oxidation state (CoHCF_{ox}) by applying cyclic potential scanning (Fig. 5, inset) in 0.5 M KCl solution. 15 voltammetric cycles from +0.9 V to +0.1 V (*vs* Ag|AgCl, KCl_{sat}) were applied to the glass|ITO| CoHCF_{ox} | $\text{KCl}_{\text{cycled}}$ electrode. Optical absorption spectra of the glass|ITO| CoHCF_{ox} | $\text{KCl}_{\text{cycled}}$ electrode recorded before investigation in H_2O_2 solution and after the electrochemical regeneration have the same form (Fig. 10B). Therefore, the decrement in CoHCF_{ox} optical absorption spectrum caused by H_2O_2 (Fig. 10B) should be clearly attributed to the reduction of the CoHCF_{ox} layer. Furthermore, reduction of CoHCF_{ox} layer, caused by CoHCF_{ox} chemical reaction with H_2O_2 , corresponds to earlier investigations [37,38] indicating the electrocatalytic activity of CoHCF towards the oxidation of H_2O_2 .

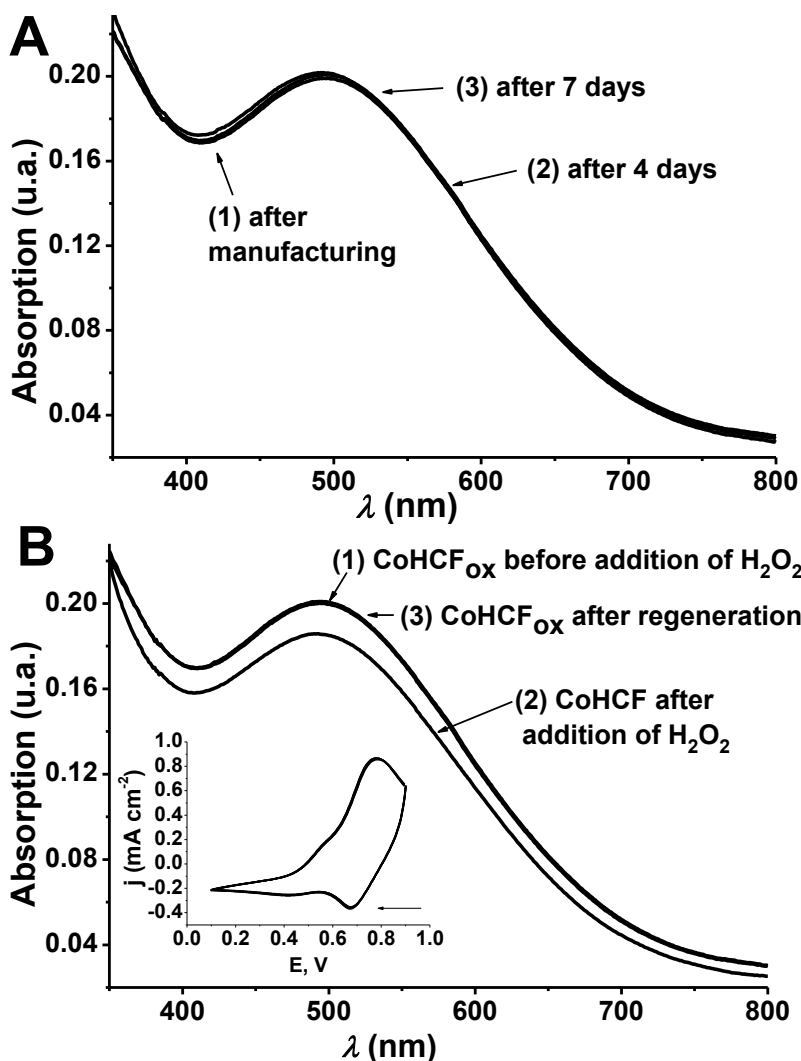


Fig. 10. **A** – optical absorption spectra of the glass|ITO|CoHCF_{ox}|KCl_{cycled} electrode measured during 7 days lasting exposition to the air. Optical absorption spectra were recorded (1) immediately after manufacturing the glass|ITO|CoHCF_{ox} electrode, (2) after 4 days, (3) after 7 days lasting exposition to the air. **B** – optical absorption spectra of the glass|ITO|CoHCF_{ox}|KCl_{cycled} electrode in 0.5 M KCl solution registered (1) before the addition of H₂O₂, (2) after the addition of 20 mM H₂O₂, (3) after the electrochemical regeneration procedure. Inset – cyclic voltammograms, registered during regeneration of the glass|ITO|CoHCF electrode in 0.5 M KCl solution.

The H_2O_2 -caused decrease in the glass|ITO|CoHCF_{ox}|KCl_{cycled} electrode optical absorption maximum appeared to be dependent on H_2O_2 concentration in 0.5 M KCl solution (Fig. 11). The decrease in absorption maximum (ΔA) of CoHCF layer was evaluated by subtracting the value of absorption maximum, recorded 5 minutes after the addition of H_2O_2 into 0.5 M KCl solution, from the initial value of the absorption maximum. (Fig. 11). Linear dependency ($R^2 = 0.990$) of ΔA on H_2O_2 concentration (Fig. 11) was obtained in the range from 1.5 mM to 20 mM with sensitivity of 8.82 u.a. M^{-1} .

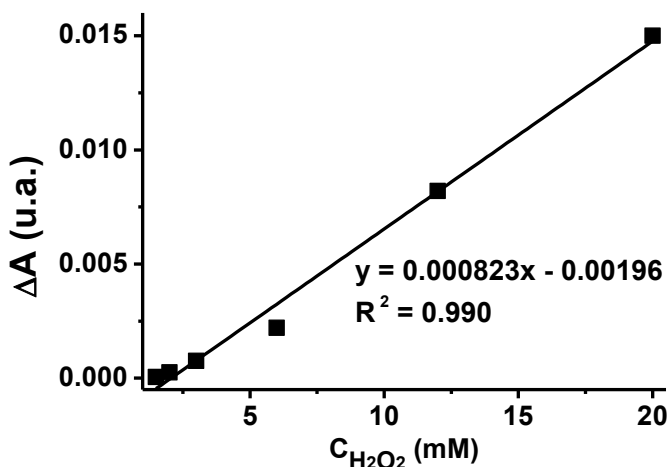


Fig. 11. Linear relation between H_2O_2 concentration (mM) and H_2O_2 -caused decrement in glass|ITO|CoHCF_{ox}|KCl_{cycled} absorption maximum (ΔA).

For a sake of comparison, earlier developed electrochemical H_2O_2 sensing techniques based on CoHCF [37,38] exhibited linear ranges of H_2O_2 concentration up to 1.2 – 9.0 mM, thus, the glass|ITO|CoHCF_{ox}|KCl_{cycled} electrode developed in this work can be applied to detect significantly higher concentrations of H_2O_2 (up to 20 mM). However, electrochemical CoHCF-based H_2O_2 sensors have achieved very low limit of H_2O_2 detection (7 – 700 nM) [37,38], and the limit of H_2O_2 detection achieved by the glass|ITO|CoHCF_{ox}|KCl_{cycled} electrode manufactured in this work is 1.5 mM. Therefore, in comparison to CoHCF-based electrochemical H_2O_2 sensing techniques [37,38], the glass|ITO|CoHCF_{ox}|KCl_{cycled} electrode is more suitable for determining higher H_2O_2 concentrations.

3.4. Investigation of the PB-modified amperometric Hg^{2+} ion biosensor based on glucose oxidase inhibition (glass|FTO|PB|GOx)

3.4.1. The principle of the glass|FTO|PB|GOx biosensor operation

The schematic representation of the principle of the glass|FTO|PB|GOx biosensor operation is shown in figure 12. The principle of the glass|FTO|PB|GOx biosensor operation is based on measuring Hg^{2+} ion-caused changes in reduction current of H_2O_2 which is a product of GOx-catalysed glucose oxidation reaction. An addition of glucose into PBS results in formation of hydrogen peroxide which is electrochemically reduced due to electrocatalytic activity of PB [10,19,40]. However, an addition of Hg^{2+} ions into PBS results in inhibition of GOx [44,46,47], thus, concentration of H_2O_2 decreases due to the presence of Hg^{2+} ions, resulting in decreased H_2O_2 reduction current (Fig. 12).

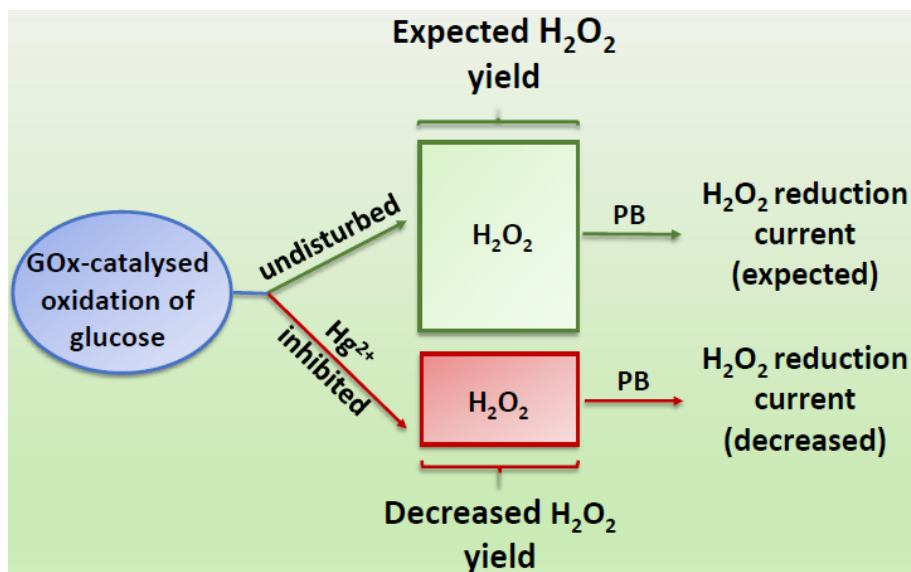


Fig. 12. Representation of the glass|FTO|PB|GOx biosensor operation.

3.4.2. Optimisation of potentiostatic conditions

Prior to investigating the glass|FTO|PB|GOx biosensor in Hg^{2+} -containing solution, amperometry-based investigation of the glass|FTO|PB electrode were conducted in PBS to determine the potential (*vs* Ag|AgCl, KCl_{sat}) optimal for the operation of the glass|FTO|PB|GOx biosensor. In order to select the potential for the operation of the glass|FTO|PB|GOx biosensor, two

main conditions should be maintained – i) the potential has to be low enough for the hydrogen peroxide reduction reaction to occur; ii) Hg^{2+} ion should not be reduced at the working electrode to ensure that the amperometric signal of the biosensor is related only to the changes in H_2O_2 concentration. It is known from earlier investigations that PB exhibits electrocatalytic properties in reduction of H_2O_2 solely in its reduced state (PW) at potentials lower than +0.15 V – +0.27 V *vs* Ag|AgCl, KCl_{sat} , depending on the electrode material and/or composition of electrolyte [10,36,71,72]. Therefore, in this research the glass|FTO|PB electrode was investigated amperometrically at the potentials of +0.15 V, +0.20 V and +0.25 V (*vs* Ag|AgCl, KCl_{sat}), and the influence of both reactants (Hg^{2+} and H_2O_2) on chronoamperometric signal was tested accordingly (Fig. 13).

Amperometric investigations of the glass|FTO|PB electrode indicated that potentials of +0.15 V (Fig. 3A) and +0.25 V (Fig. 13B) are not suitable for the operation of Hg^{2+} biosensor. At +0.15 V potential reduction of Hg^{2+} ions was observed (Fig. 13A), while application of +0.25 V to the glass|FTO|PB electrode resulted in rather weak amperometric response to H_2O_2 (Fig. 13B). Sufficient H_2O_2 reduction current and no electrochemical response to Hg^{2+} ions were obtained when potential of +0.2 V (*vs* Ag|AgCl, KCl_{sat}) was applied to the glass|FTO|PB electrode (Fig. 13C). During the amperometric investigation of the glass|FTO|PB electrode at +0.2 V potential, cathodic current reached a constant value ($\sim 0 \mu\text{A cm}^{-2}$) within the first 200 s of the experiment. An addition of Hg^{2+} ions (Fig. 13C, approximately at 700 s) did not cause amperometric signal, indicating that reduction of Hg^{2+} does not occur when potential of +0.2 V is applied to the electrode. However, an addition of H_2O_2 (Fig. 13C, approximately at 1100 s) caused an increase in cathodic current from $\sim 0 \mu\text{A cm}^{-2}$ to $- 45 \mu\text{A cm}^{-2}$, proving that electrochemical reduction of H_2O_2 takes place when +0.2 V (*vs* Ag|AgCl, KCl_{sat}) potential is applied to the glass|FTO|PB electrode. Therefore, potential of +0.2 V was used in further chronoamperometric investigations of a GOx inhibition-based Hg^{2+} ion biosensor (glass|FTO|PB|Gox).

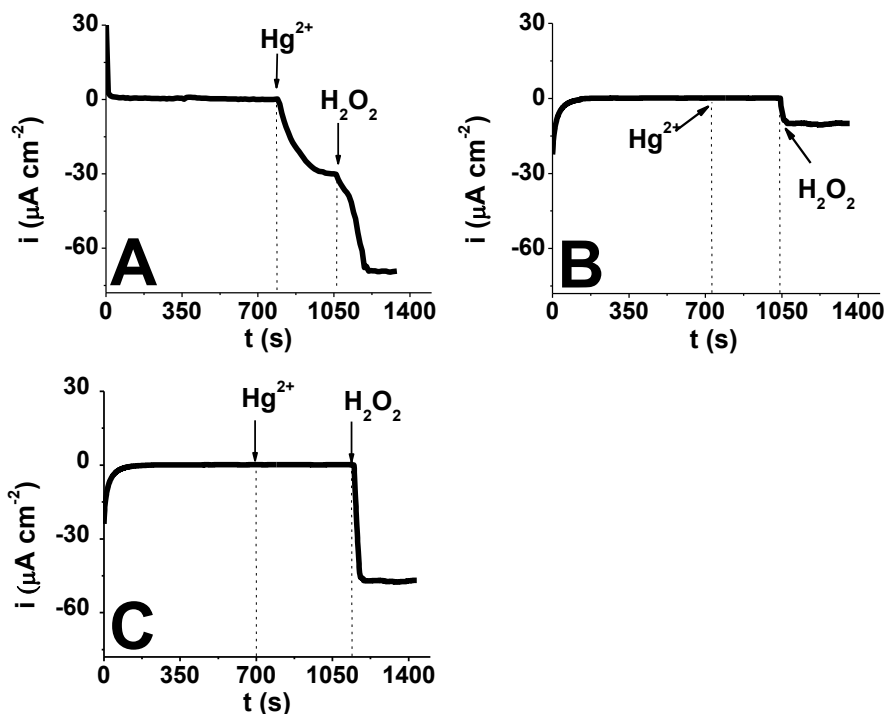


Fig. 13. Chronoamperometric investigations of the glass|FTO|PB electrode in PBS performed at (A) +0.15 V, (B) +0.25 V and (C) +0.2 V (vs Ag|AgCl, KCl_{sat}) potential. Chronoamperograms were registered by adding 0.3 mM of Hg^{2+} into PBS at approx. 700 s after the beginning of experiment to register the Hg^{2+} caused current responses and then, 0.3 mM of H_2O_2 was added at approx. 1100 s to register the H_2O_2 caused current responses.

3.4.3. Amperometric investigation of the glass|FTO|PB|GOx biosensor

Amperometric investigation of the glass|FTO|PB|GOx biosensor was performed by adding 1.3 mM of glucose and various concentrations (from 27 μM to 247 μM) of Hg^{2+} ions into PBS. During this investigation +0.2 V (vs Ag|AgCl, KCl_{sat}) potential was applied to the glass|FTO|GOx biosensor. Glucose concentration of 1.3 mM appeared to be optimal for operation of biosensor, since lower glucose concentrations resulted in lower reduction current of H_2O_2 , while glucose concentrations higher than 1.3 mM resulted in unstable amperometric response. An example of amperometric investigation of the glass|FTO|PB|GOx biosensor performed by adding 1.3 mM of glucose and 247 μM of Hg^{2+} into PBS is given in Fig. 14B. After the addition of glucose into PBS, an increase in reduction current (Fig. 14A) was observed

due to production of H_2O_2 during GOx-catalysed oxidation of glucose (Eq. 12) [10,19,40,73].



Meanwhile, a decrement in reduction current was observed after adding Hg^{2+} ions into PBS (Fig. 14A), indicating the GOx inhibition by Hg^{2+} ions.

The glass|FTO|PB|GOx biosensor could be used for several investigations in Hg^{2+} -containing solution, since Hg^{2+} ions-affected GOx can be regenerated with EDTA [74]. However, it was determined [74] that regeneration of the glass|FTO|GOx biosensor with EDTA solution (0.1 M) has a limited efficiency - after the regeneration procedure, amperometric response of the glass|FTO|PB|GOx biosensor to 1.3 mM of glucose decreased by approximately 28 %. This decrement in GOx activity (approx. 28 %) goes in line with ~ 0 % – 24 % decrease in Hg^{2+} ion-affected GOx activity after regeneration mentioned in earlier publications [44,45,75]. Nevertheless, to ensure high reliability of the measurement, current response of the glass|FTO|PB|GOx biosensor to each concentration of Hg^{2+} was evaluated using freshly prepared glass|FTO|PB|GOx biosensor. Linear dependency of Hg^{2+} -caused decrement in H_2O_2 reduction current (dj , %) on concentration of Hg^{2+} ions was observed in rather wide range from 27 μM to 247 μM of Hg^{2+} (Fig. 14B). In comparison, other Hg^{2+} ion biosensors based on GOx inhibition [44-47,76] exhibited linear ranges of Hg^{2+} concentration varying between 0.025 μM and 180 μM (Table 2). Furthermore, in this research developed glass|FTO|PB|GOx biosensor was able to detect higher Hg^{2+} concentrations than other GOx inhibition-based biosensors (Table 2). Detection of high Hg^{2+} concentrations could be convenient for analysis of samples containing higher concentration of mercury e.g., extracts made from soil or sediments [77-80]. Another advantageous feature of the glass|FTO|PB|GOx biosensor is ability to operate at +0.2 V (*vs* Ag|AgCl, KCl_{sat}) potential that is significantly lower than +0.4 V – +0.7 V (*vs* Ag|AgCl, KCl_{sat}) potentials used in operation of earlier developed amperometric GOx inhibition-based Hg^{2+} ion biosensors (Table 2). Application of such low electrode potential (+0.2 V *vs* Ag|AgCl, KCl_{sat}) enables to avoid some side electrochemical reactions (e.g., oxidation of sulfite or some alkylphenols [48-50]) that could occur during the measurement of Hg^{2+} ions concentration.

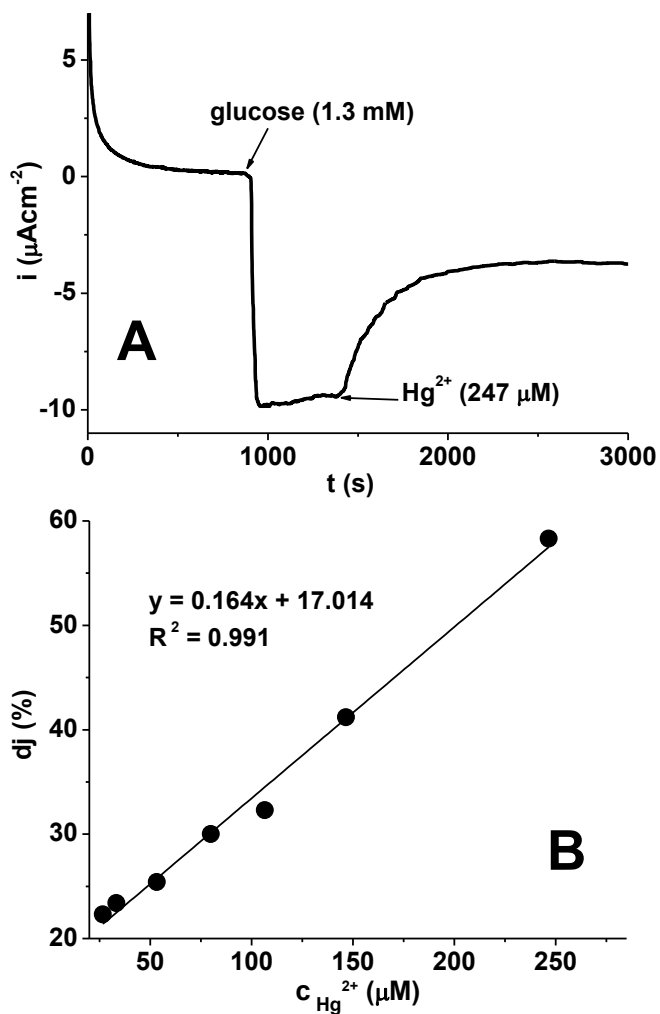


Fig. 14. **A** – an example of amperometric investigation of the glass|FTO|PB|GOx biosensor. **B** – linear dependency of Hg^{2+} -caused decrement in H_2O_2 reduction current (dj) on concentration of Hg^{2+} ions.

Table 2. Operating conditions and linear ranges of electrochemical GOx inhibition-based Hg²⁺ ion biosensors

Biosensor	Electrochemical technique	Electrode potential, V (vs Ag AgCl, KCl_{sat})	Linear range, μM
GCE/MWCNTs-RuO ₂ /GOx/Nafion® [44]	Amperometry	+0.4	5 – 80
Pt/PPD/GOx [47]	Amperometry	+0.7	5 – 180
(CS/GLM) ₈ -GCE [46]	Cyclic voltammetry	-0.3 – +0.9	0.5 – 5
Pt/PPy-GOx [76]	Potentiometry	-	0.025 – 5
glass FTO PB GOx (this work)	Amperometry	+0.2	27 – 247

GENERAL CONCLUSIONS

1. Prussian blue was applied in fabrication of the electrochromic ammonium ion sensor (glass|ITO|PB). The glass|ITO|PB sensor exhibited linear range from 0.01 M to 0.1 M with sensitivity of 0.35 u.a. M^{-1} .
2. The electrochromic urea biosensor was developed by coating the glass|ITO electrode with Prussian blue layer and immobilising an enzyme urease (glass|ITO|PB|urease). The glass|ITO|PB|urease biosensor exhibited linear range from 3 mM to 30 mM with sensitivity of 4.2 u.a. M^{-1} .
3. Cobalt hexacyanoferrate was applied in a construction of the optical sensor for hydrogen peroxide (glass|ITO|CoHCF_{ox}|KCl_{cycled}). The glass|ITO|CoHCF_{ox}|KCl_{cycled} sensor exhibited linear range from 1.5 mM to 20 mM with sensitivity of 0.82 u.a. M^{-1} .
4. Amperometric Hg²⁺ ion biosensor was developed by coating the glass|FTO electrode with Prussian blue layer and immobilising an enzyme urease (glass|FTO|PB|urease). The glass|FTO|GOx biosensor exhibited linear range from 27 μ M to 247 μ M.

REFERENCES

1. J. F. Keggin, F. D. Miles, *Nature* **1936**, *137*, 577–578.
2. C. A. Lundgren and R. W. Murray, *Inorg. Chem.* **1988**, *27*, 933–939.
3. J. Agrisuelas, C. Delgado, C. Gabrielli, J.J. García-Jareño, H. Perrot, F. Vicente, *ECS Trans.* **2011**, *35*, 53–61.
4. A. Dostal, G. Kauschka, S. J. Reddy, F. Scholz, *J. Electroanal. Chem.* **1996**, *406*, 155–163.
5. A. Kraft, *Ionics* **2021**, *27*, 2289–2305.
6. R. J. Mortimer, in *Encyclopedia of Spectroscopy and Spectrometry* (Ed: J. C. Lindon), Elsevier, Amsterdam, **2000**, p.p. 2161–2174.
7. P. J. Kulesza, M. A. Malik, S. Zamponi, M. Berrettoni, R. Marassi, *J. Electroanal. Chem.* **1995**, *397*, 287–292.
8. P. J. Kulesza, K. Miecznikowski, M. Chojak, M. A. Malik, S. Zamponi, R. Marassi, *Electrochim. Acta* **2001**, *46*, 4371–4378.
9. J. Agrisuelas, C. Delgado, J.J. García-Jareño, C. Moreno-Guerrero, A. Roig, F. Vicente, *ECS Trans.* **2013**, *50*, 435–447.
10. A. A. Karyakin, *Electroanalysis* **2001**, *13*, 813–819.
11. M. Hermes, F. Scholz, *J. Solid State Electrochem.* **1997**, *1*, 215–220.
12. K. Itaya, I. Hida, *Acc. Chem. Res.* **1986**, *19*, 162–168.
13. P. J. Kulesza, M. A. Malik, M. Berrettoni, M. Giorgetti, S. Zamponi, R. Schmidt, R. Marassi, *J. Phys. Chem. B* **1998**, *102*, 1870–1876.
14. R. Vittal, H. Gomathi, G. P. Rao, *Electrochim. Acta* **2000**, *45*, 2083–2093.
15. A. Roig, J. Navarro, R. Tamarit and F. Vicente, *J. Electroanal. Chem.* **1993**, *360*, 55–69.
16. A. Roig, J. Navarro, J. J. Garcia, F. Vicente, *Electrochim. Acta* **1994**, *39*, 437–442.
17. J. Agrisuelas, J. J. García-Jareño, D. Gimenez-Romero, F. Vicente, *J. Electroch. Soc.* **2009**, *156*, 149–156.
18. S. Zamponi, M. Berrettoni, P. J. Kulesza, K. Miecznikowski, M. A. Malik, O. Makowski, R. Marassi, *Electrochim. Acta* **2003**, *48*, 4261–4269.
19. A. A. Karyakin, E. E Karyakina, L. Gorton, *Talanta* **1996**, *43*, 1597–1606.
20. Y. Lin, L. Hu, L. Yin, L. Guo, *Sens. Actuators B: Chem.* **2015**, *210*, 513–518.
21. B. Haghghi, M. Khosravi, A. Barati, *Mater. Sci. Eng. C* **2014**, *40*, 204–211.
22. S. Cinti, F. Arduini, D. Moscone, G. Palleschi, A. J. Killard, *Sens. (Basel)* **2014**, *14*, 14222–14234.
23. F. Ricci, G. Palleschi, *Biosens. Bioelectron.* **2005**, *21*, 389–407.

24. R. Koncki, T. Lenarczuk, A. Radomska, S. Glab, *Analyst* **2001**, *126*, 1080–1085.
25. A. Zloczewska, A. Celebanska, K. Szot, D. Tomaszewska, M. Opallo, M. Jönsson-Niedziolka, *Biosens Bioelectron.* **2014**, *54*, 455–461.
26. P. Yue, S. Tricard, S. He, N. Wang, J. Zhao, J. Fang, W. Shen, *Electroanalysis* **2016**, *28*, 1340–1347.
27. S. Cinti, F. Arduini, D. Moscone, G. Palleschi, L. Gonzalez-Macia, A. J. Killard, *Sens. Actuators B: Chem.* **2015**, *221*, 187–190.
28. J. Li, T. Peng, Y. Peng, *Electroanalysis* **2003**, *15*, 1031–1037.
29. S. Suwansa-ard, Y. Xiang, R. Bash, P. Thavarungkul, P. Kanatharana, J. Wang, *Electroanalysis* **2008**, *20*, 308–312.
30. Y. Matos-Peralta, M. Antuch, *J. Electrochem. Soc.* **2020**, *167*, 037510.
31. S. Jankovskaja, A. Labrousse, L. Prévaud, B. Holmqvist, A. Brinte, J. Engblom, M. Rezeli, G. Marko-Varga, T. Ruzgas, *Microchim. Acta* **2020**, *187*, 656.
32. T. Lenarczuk, D. Wencel, S. Głab, R. Koncki. *Anal. Chim. Acta* **2001**, *447*, 23–32.
33. D. O. Ojwang, M. Svensson, C. Njel, R. Mogensen, A. S. Menon, T. Ericsson, L. Häggström, J. Maibach, W. R. Brant, *ACS Appl. Mater. Interfaces* **2021**, *13*, 10054–10063.
34. P. Virbickas, A. Valiūnienė, G. Kavaliauskaitė, A. Ramanavicius, *J. Electrochem. Soc.* **2019**, *166*, B927–B932.
35. M. Hu, J. S. Jiang, *Mater. Res. Bulletin* **2011**, *46*, 702–707.
36. A. A. Karyakin, *Curr. Opin. Electrochem.* **2017**, *5*, 92–98.
37. Z. Hong-Cai, Z. Pu, L. She-Hong, L. Hong-Xia, *Chin. J. Anal. Chem.* **2017**, *45*, 830–836.
38. Y. Ye, Y. Zheng, J. Yu, Y. Zhang, Y. Song, Q. Guo, L. Wang, F. Xu, *Anal. Methods* **2016**, *8*, 2666–2672.
39. K. Itaya, N. Shoji, I. Uchida, *J. Am. Chem. Soc.* **1984**, *106*, 3423–3429.
40. A. Ramanavicius, A. I. Rekertaitė, R. Valiūnas, A. Valiūnienė, *Sens. Actuators B: Chem.* **2017**, *240*, 220–223.
41. F. Charmantray, N. Touisni, L. Hecquet, T. Noguer, C. Mousty, *Electroanalysis*, **2015**, *27*, 1341–1344.
42. X. Wang, H. Gu, F. Yin, Y. Tu, *Biosens. Bioelectron.* **2009**, *24*, 1527–1530.
43. R. Garjonyte, A. Malinauskas, *Biosens. Bioelectron.* **2000**, *15*, 445–451.
44. A. M. Ashrafi, M. Sýs, E. Sedláčková, A. S. Farag, V. Adam, J. Příbyl, L. Richtera, *Sens. (Basel)* **2019**, *19*, 2939.
45. C. Malitesta, M. R. Guascito, *Biosens. Bioelectron.* **2005**, *20*, 1643–1647.
46. J. Yu, H. Guan, D. Chi, *J. Solid State Electrochem.* **2017**, *21*, 1175–1183.

47. M. R. Guascito, C. Malitesta, E. Mazzotta, A. Turco, *Sens. Actuators B: Chem.* **2008**, *131*, 394–402.
48. A. Chmayssem, D. Hauchard, *J. Water Sci.* **2015**, *28*, 35–40.
49. O. N. Novgorodtseva, A. Zelinsky, *J. Solid State Electrochem.* **2019**, *23*, 2301–2306.
50. C. A. Martínez-Huitle, M. Panizza, *Curr. Opin. Electrochem.* **2018**, *11*, 62–71.
51. H. Düssel, A. Dostal, F. Scholz, *Fresenius J. Anal. Chem.* **1996**, *355*, 21–28.
52. M. A. Pellitero, F. J. Campo, *Curr. Opin. Electrochem.* **2019**, *15*, 66–72.
53. J. J. García-Jareño, A. Sanmatías, J. Navarro-Laboulais, F. Vicente, *Electrochim. Acta* **1998**, *44*, 395–405.
54. J. J. García-Jareño, J. Navarro-Laboulais, F. Vicente, *Electrochim. Acta* **1996**, *41*, 835–841.
55. A. Valiūnienė, G. Kavaliauskaitė, P. Virbickas, A. Ramanavičius, *J. Electroanal. Chem.* **2021**, *895*, 115473.
56. R. Koncki, O. S. Wolfbeis, *Anal. Chem.* **1998**, *70*, 2544–2550.
57. R. Koncki, O. S. Wolfbeis, *Biosens. Bioelectron.* **1999**, *14*, 87–92.
58. G. Dhawan, G. Sumana, B. D. Malhotra, *Biochem. Eng. J.* **2009**, *44*, 42–52.
59. N. A. Sitnikova, A. V. Borisova, M. A. Komkova, A. A. Karyakin, *Anal. Chem.* **2011**, *83*, 2359–2363.
60. R. J. Kulesza, M. A. Malik, K. Miecznikowski, A. Wolkiewicz, *J. Electrochem. Soc.* **1996**, *143*, L10.
61. R. O. Lezna, R. Romagnoli, N. R. de Tacconi, K. Rajeshwar, *J. Phys. Chem. B* **2002**, *106*, 3612–3621.
62. J. J. Garcia-Jareno, J. Navarro-Laboulais, F. Vicente, *Electrochim. Acta.* **1997**, *42*, 1473–1480.
63. M. Berrettoni, M. Giorgetti, S. Zamponi, P. Conti, D. Ranganathan, A. Zanotto, M. L. Saladino, E. Caponetti, *J. Phys. Chem. C* **2010**, *114*, 6401–6407.
64. O. Barbosa, C. Ortiz, Á. Berenguer-Murcia, R. Torres, R. C. Rodrigues, R. Fernandez-Lafuente, *RSC Adv.* **2014**, *4*, 1583–1600.
65. P. Virbickas, A. Valiūnienė, A. Ramanavičius, *Electrochem. Commun.* **2018**, *94*, 41–44.
66. R. J. Mortimer, D. R. Rosseinsk, *J. Chem. Soc. Dalton Trans.* **1984**, 2059–2061.
67. C. S. Pundir, S. Jakhar, N. Vinay, *Biosens. Bioelectron.* **2019**, *123*, 36–50.
68. B. Krajewska, Ureasas I. Functional, *J. Mol. Catal. B* **2009**, *59*, 9–21.

69. A. Valiūnienė, P. Virbickas, G. Medvikytė, A. Ramanavičius, *Electroanalysis* **2020**, *32*, 503–509.
70. P. Virbickas, G. Kavaliauskaitė, A. Valiūnienė, V. Plaušinitienė, A. I. Rekertaitė, A. Ramanavičius, *Electrochim. Acta* **2020**, *362*, 137202.
71. K. Itaya, H. Akahoshi, *J. Electrochem. Soc.* **1982**, *129*, 1498–1500.
72. A. Valiūnienė, P. Virbickas, G. Medvikytė, A. Ramanavičius, *Electroanalysis* **2020**, *32*, 503–509.
73. N. Suzuki, J. Lee, N. Loew, Y. Takahashi-Inose, J. Okuda-Shimazaki, K. Kojima, K. Mori, W. Tsugawa, K. Sode, *Int. J. Mol. Sci.* **2020**, *21*, 1137.
74. P. Virbickas, G. Ziziunaite, A. Ramanavicius, A. Valiūnienė, *Electroanalysis* **2022**, *34*.
75. A. Samphao, H. Rerkchai, J. Jitcharoen, D. Nacapricha, K. Kalcher, *Int. J. Electrochem. Sci.* **2012**, *7*, 1001–1010.
76. J. G. Ayenimo, S. B. Adeloju, *Talanta* **2015**, *137*, 62–70.
77. A. S. Maghsoudi, S. Hassani, K. Mirnia, M. Abdollahi, *Int. J. Nanomed.* **2021**, *16*, 803–832.
78. J. E. Gray, P. M. Theodorakos, D. L. Fey, D. P. Krabbenhoft, *Environ. Geochem. Health* **2015**, *37*, 35–48.
79. A. Bernaus, X. Gaona, D. van Ree, M. Valiente, *Anal. Chim. Acta* **2006**, *565*, 73–80.
80. L. D. Hylander, M. Meili, *Sci. Total Environ.* **2003**, *304*, 13–27.

SANTRAUKA

ĮVADAS

Berlyno mėlynasis (PB) ir jo struktūriniai analogai (PBSA), pvz.: kobalto heksacianoferatas (CoHCF), yra neorganiniai pigmentai, turintys platų pritaikymą cheminės analizės srityje. Vieni pagrindinių PB ir PBSA privalumų yra tai, kad cheminiai ir biologiniai jutikliai, suformuoti panaudojant PB ir/arba PBSA, pasižymi maža savikaina ir galimybe naudoti žemą ($\sim 0 \text{ V vs Ag|AgCl, KCl}_{\text{sat.}}$) darbinio elektrodo potencialą analizės metu. Žemas ($\sim 0 \text{ V vs Ag|AgCl, KCl}_{\text{sat.}}$) darbinio elektrodo potencialas yra naudingas tuo, kad sumažina elektrochemiškai aktyvių medžiagų, kurios gali būti aptinkamos tiriamajame mėginyje, elektrocheminės oksidacijos įtaką analizės patikimumui.

Amonio jonų (arba amoniako), Hg^{2+} jonų, karbamido ir vandenilio peroksido koncentracijos tyrimai yra aktualūs tiek sveikatos priežiūros, tiek aplinkosaugos srityse. Vis dėlto, nepaisant galimo PB ir PBSA efektyvumo gerinant analizinių sistemų savybes, iki šiol nebuvo atlikta tyrimų, kurie analizuotų PB pritaikomumą elektrochrominiam amonio jonų ir karbamido nustatymui, PB tinkamumą sunkiųjų metalų detekcijai per fermentų inhibiciją ir CoHCF pritaikomumą optiniam vandenilio peroksido nustatymui. PB ir/arba PBSA pritaikymas minėtiesiems tyrimams (vandenilio peroksido, amonio jono, karbamido, sunkiųjų metalų jonų nustatymui) potencialai galėtų pagerinti esamų analizės sistemų charakteristikas, pvz.: praplėsti nustatomų koncentracijų ribas; užtikrinti didesnę jutiklio atsparumą pašalinių elektrochemiškai aktyvių medžiagų buvimo analizuojamame mėginyje atveju; padidinti jutiklio inertiškumą tokių faktorių, kaip mėginio buferinė talpa arba oksiduojantis deguonies poveikis, atžvilgiu.

Darbo tikslas:

Naudojant Berlyno mėlynąjį ir/arba kobalto heksacianoferatą suformuoti jutiklius amonio jonų, karbamido, vandenilio peroksido ir Hg^{2+} jonų nustatymui.

Darbo uždaviniai:

1. Suformuoti elektrochrominį amonio jonų jutiklį, padengiant indžio-alavo oksidu modifikuoto stiklo elektrodą (glass|ITO) Berlyno mėlynuoju; iširti suformuoto jutiklio elektrochrominį atsaką į skirtingas amonio jonų koncentracijas tirpale.

2. Suformuoti elektrochrominį biologinį karbamido jutiklį, padengiant glass|ITO elektrodą PB sluoksniu ir fiksuojant fermentą ureazę PB dangos paviršiuje (glass|ITO|PB|urease); ištirti elektrochrominį biologinio jutiklio atsaką į skirtingas karbamido koncentracijas tirpale.
3. Sukurti optinį vandenilio peroksido jutiklį padengiant glass|ITO elektrodą oksiduoto kobalto heksacianoferato (CoHCF_{ox}) sluoksniu; parinkti optimalias sąlygas elektrochrominio virsmo tarp oksiduoto ir redukuoto CoHCF būvių stebėjimui; ištirti suformuoto jutiklio optinį atsaką į skirtingas vandenilio peroksido koncentracijas tirpale.
4. Suformuoti elektrocheminį Hg^{2+} jonų jutiklį padengiant fluoru legiruotu alavo oksidu modifikuotu stiklo elektrodą (glass|FTO) PB sluoksniu (glass|FTO|PB) ir fiksuojant fermentą gliukozės oksidazę (GOx) PB dangos paviršiuje (glass|FTO|PB|GOx); nustatyti potencialą, optimalų sukurto biologinio jutiklio veikimui; ištirti amperometrinį biologinio jutiklio atsaką į skirtingas Hg^{2+} jonų koncentracijas tirpale.

Mokslinis naujumas:

Siekiant keisti ir tobulinti esamų analizinių sistemų, pvz.: cheminių ir biologinių jutiklių, charakteristikas, tokias kaip tyrimo atrankumas ir tiesinis koncentracijų intervalas, daug mokslinių tyrimų atliekama tobulinant jutiklių sudėtį, išbandant naujas medžiagas analičių nustatymui. To pavyzdys gali būti Berlyno mėlynasis, kuris cheminės analizės srityje buvo pradėtas naudoti dėl savo jautrumo vandenilio peroksidui, o vėliau jo pritaikymas išsiplėtė iki elektrocheminio jonų nustatymo, optinio ir elektrocheminio pH pokyčių nustatymo, elektrocheminio askorbo rūgšties koncentracijos nustatymo ir kitų pritaikymų. Nemažai dėmesio susilaukė ir Berlyno mėlynojo struktūriniai analogai, tokie, kaip Co ir Ni heksacianoferatai, kurie buvo sėkmingai pritaikyti elektrocheminiam vandenilio peroksido nustatymui bei Berlyno mėlynojo dangos ilgaamžiškumo ir stabilumo didinimui.

Šio darbo metu Berlyno mėlynasis buvo pirmą kartą panaudotas elektrochrominiam amonio jonų ir karbamido koncentracijos nustatymui, taip pat elektrocheminiam Hg^{2+} jonų nustatymui, o Berlyno mėlynojo struktūrinis analogas – kobalto heksacianoferatas – buvo pirmą kartą panaudotas optiniam vandenilio peroksido nustatymui. Pagrindiniai moksliniai ir praktiniai pasiekimai, įgyvendinti atliekant šį darbą, yra:

1. Nustatyta, kad PB gali būti naudojamas elektrochrominiam amonio jonų nustatymui, o ureaze modifikuota PB danga gali būti naudojama elektrochrominiam karbamido nustatymui

2. Nustatyta, kad karbamido nustatymas glass|ITO|PB|urease biologiniu jutikliu, kurio sudėtyje panaudota K^+ jonais praturtinta PB forma, yra nesusijęs su PB dangos šarminė hidrolize, todėl glass|ITO|PB|urease biologinis jutiklis yra mažiau jautrus analizuojamo mėginio buferinės talpos pokyčiams, nei anksčiau suformuoti K^+ jonais nepraturtintos PB dangos šarminės hidrolizės principu veikiantys biologiniai karbamido jutikliai.
3. Berlyno mėlynojo struktūrinis analogas – kobalto heksacianoferatas – buvo pirmą kartą panaudotas optiniam vandenilio peroksido nustatymui. Nustatyta, kad oksiduota kobalto heksacianoferato forma ($CoHCF_{ox}$), kitaip nei optiniam vandenilio peroksido nustatymui iki šiol naudotas Berlyno baltasis, yra atspari oro deguonies poveikiui, todėl ore esantis deguonis negali paveikti $CoHCF_{ox}$ jautrumo vandenilio peroksidui.
4. Berlyno mėlynasis buvo pirmą kartą pritaikytas amperometriniam Hg^{2+} jonų nustatymui per gliukozės oksidazės inhibiciją. Dėl Berlyno mėlynojo panaudojimo GOx inhibicijos pagrindu veikiančiame Hg^{2+} jonų biologiniame jutiklyje, šio darbo metu suformuotas Hg^{2+} jonų jutiklis veikė darbiniam elektrodai suteikęs santykinai žemą +0,2 V (vs Ag|AgCl, $KCl_{sot.}$) potencialą, kuris yra žemesnis, nei +0,4 - +0,7 V (vs Ag|AgCl, $KCl_{sot.}$) potencialai, iki šiol naudoti gliukozės oksidazės inhibicijos pagrindu veikiančių amperometrinių biologinių Hg^{2+} jonų jutiklių veikimui. Žemo potencialo suteikimas darbiniam elektrodai analizės metu padeda išvengti kai kurių kitų mėginyje esančių junginių (pvz.: alkilfenolių) elektrocheminės oksidacijos reakcijų, taip padidinant analizės patikimumą.

Ginamieji teiginiai:

1. Berlyno mėlynasis gali būti pritaikomas elektrochrominiam amonio jonų koncentracijos nustatymui.
2. Biologinis jutiklis, suformuotas padengiant glass|ITO elektrodą Berlyno mėlynojo sluoksniu ir fiksavus fermentą ureazę Berlyno mėlynojo dangos paviršiuje, gali būti naudojamas elektrochrominiam karbamido koncentracijos nustatymui.
3. Kobalto heksacianoferatas gali būti naudojamas optiniam vandenilio peroksido nustatymui.
4. Biologinis jutiklis, suformuotas padengiant glass|FTO Berlyno mėlynojo sluoksniu ir fiksavus fermentą gliukozės oksidazę Berlyno mėlynojo dangos paviršiuje, gali būti naudojamas amperometriniam Hg^{2+} jonų nustatymui.

EKSPERIMENTŲ METODIKA

Elektrocheminis Berlyno mėlynojo ir kobalto heksacianoferato sluoksnių formavimas

Berlyno mėlynojo (PB) sluoksniai buvo elektrochemiškai suformuoti ant glass|ITO ir glass|FTO elektrodų iš tirpalo, sudaryto iš 1 mM $\text{FeCl}_3 \cdot 6\text{H}_2\text{O}$ ir 1 mM $\text{K}_3[\text{Fe}(\text{CN})_6]$. Formuojant biologinius jutiklius Hg^{2+} jonams ir karbamidui, į nusodinimo tirpalą buvo papildomai pridėta 0,1 M HCl, nes rūgštinė terpė padeda išvengti defektų susidarymo PB kristalinėje gardelėje [10,36]. Elektrocheminis PB nusodinimas atliktas taikant ciklinį potencialo skleidimą (40 ciklų) intervale nuo +0,4 V iki +0,8 V (vs Ag|AgCl, $\text{KCl}_{\text{sat.}}$), esant 40,0 mV s^{-1} potencialo skleidimo greičiui. Nusodinus PB dangas, jos buvo elektrochemiškai stabilizuotos panaudojant ciklinę voltamperometriją 0,1 M KCl tirpale. Formuojant biologinius jutiklius Hg^{2+} jonams ir karbamidui, į KCl (0,1 M) tirpalą papildomai buvo pridėta 0,1 M HCl. Elektrocheminis PB stabilizavimas atliktas pasitelkus ciklinį potencialo skleidimą (20 voltamperinių ciklų) intervale nuo $0 \pm 0,05$ V iki $+0,45 \pm 0,05$ V (vs Ag|AgCl, $\text{KCl}_{\text{sat.}}$), esant 40,0 mV s^{-1} potencialo skleidimo greičiui. Glass|ITO|PB elektrodas, turintis elektrochemiškai stabilizuotą PB sluoksnį, buvo naudojamas kaip elektrochrominis amonio jonų jutiklis.

Kobalto heksacianoferato (CoHCF) sluoksnis nusodintas ant glass|ITO elektrodų naudojant ciklinės voltamperometrijos pagrindu veikiančią nusodinimo procedūrą [60,61]. Azoto dujomis nudeguonintas nusodinimo tirpalas buvo sudarytas iš $\text{CoCl}_2 \cdot 6\text{H}_2\text{O}$ (1 mM), $\text{K}_3[\text{Fe}(\text{CN})_6]$ (1 mM) ir KCl (500 mM). CoHCF sluoksnio nusodinimui ant glass|ITO elektrodo (glass|ITO|CoHCF) panaudotas ciklinis potencialo skleidimas (60 voltamperinių ciklų) nuo +0,1 V iki +0,9 V (vs Ag|AgCl, $\text{KCl}_{\text{sat.}}$), potencialo skleidimo greitis 50,0 mV s^{-1} . Norint gauti oksiduoto būvio CoHCF dangą (glass|ITO|CoHCF_{ox} elektrodas), ciklinis potencialo skleidimas buvo stabdomas ties +0,9 V (vs Ag|AgCl| $\text{KCl}_{\text{sat.}}$). Atsižvelgiant į tai, kad ciklinis potencialo skleidimas K^+ jonų turinčiame tirpale pagerina CoHCF struktūrinio analogo – PB – elektrochemines savybes, šio darbo metu glass|ITO|CoHCF elektrodas taip pat buvo paveiktas cikline voltamperometrija KCl tirpale: glass|ITO|CoHCF elektrodai suteikta 15 voltamperinių ciklų nuo +0,9 V iki +0,1 V (vs Ag|AgCl, $\text{KCl}_{\text{sat.}}$) 0,5 M KCl tirpale (potencialo skleidimo greitis 50,0 mV s^{-1}), taip suformuojant glass|ITO|CoHCF_{ox}| $\text{KCl}_{\text{cycled}}$ elektrodą, naudotą optiniam vandenilio peroksido nustatymui.

Fermentų fiksavimas Berlyno mėlynojo dangos paviršiuje

Formuojant biologinius karbamido ir Hg^{2+} jonų jutiklius, ant elektrochemiškai stabilizuotų PB sluoksnių buvo fiksuojami fermentai ureazė ir gliukozės oksidazė (GOx). Ureazė buvo užnešta ant glass|ITO|PB elektrodo, taip suformuojant glass|ITO|PB|urease biologinį jutiklį karbamidui, o GOx buvo užnešta ant glass|FTO|PB elektrodo, suformuojant glass|FTO|PB|GOx biologinį jutiklį Hg^{2+} jonų nustatymui. Fiksuojant ureazę glass|ITO|PB elektrodo PB dangos paviršiuje, 7 μL ureazės tirpalo (20 mg mL^{-1}) buvo tolygiai paskirstyta ant glass|ITO|PB elektrodo PB sluoksnio (0,7 cm^2 geometrinis plotas), išdžiovinta kambario sąlygomis, o vėliau 15 minučių paveikta gliutaro aldehido tirpalo (25 %) garais. Panaši procedūra pasitelkta fiksuojant GOx ant glass|FTO|PB elektrodo PB sluoksnio: 15 μL 15 mg mL^{-1} GOx tirpalo buvo paskirstyta ant PB sluoksnio paviršiaus (1 cm^2 geometrinis plotas) ir palikta išdžiūti kambario sąlygomis; GOx imobilizavimas baigtas paveikiant fermentu padengtą elektrodą gliutaro aldehido tirpalo (25 %) garais 15 min.

Elektrochromio amonio jonų jutiklio (glass|ITO|PB elektrodo) tyrimai

Glass|ITO|PB elektrodas buvo tiriamas skaidraus stiklo kiuvetėje, užpildytoje vandeniniu 0,01 M – 0,1 M NH_4Cl tirpalu. Absorbcijos spektrų registravimo metu glass|ITO|PB elektrodai buvo suteikiamas +0,2 V (vs $\text{Ag}|\text{AgCl}, \text{KCl}_{\text{sat.}}$) potencialas.

Elektrochrominio karbamido jutiklio (glass|ITO|PB|urease) tyrimai

Glass|ITO|PB|urease biologinis jutiklis buvo tiriamas skaidraus stiklo kiuvetėje, užpildytoje fosfatinio buferiniu tirpalu (PBS), pH 5,5, ir pridėdant į PBS (pH 5,5) įvairias karbamido koncentracijas (nuo 3 mM iki 30 mM). Karbamido sukeltų glass|ITO|PB|urease biologinio jutiklio optinių savybių pokyčių tyrimo metu jutikliui suteiktas pastovus +0,2 V (vs $\text{Ag}|\text{AgCl}, \text{KCl}_{\text{sat.}}$) potencialas. Absorbcijos spektrai buvo registruojami praėjus 2 min. nuo karbamido įlašavimo į PBS. Tarp tyrimų skirtingas karbamido koncentracijas turinčiuose PBS, biologinis jutiklis buvo regeneruojamas įmerkiant jį į PBS (pH 5,5) vienai minutei.

Tiriant pH įtaką glass|ITO|PB|urease biologinio jutiklio optinėms savybėms, prieš absorbcijos spektro registravimą, glass|ITO|PB|urease jutiklis buvo panardinamas į PBS su tam tikra pH verte (nuo 5,5 iki 12) ir palaikomas PBS 2 min. Šio tyrimo metu glass|ITO|PB|urease biologiniam jutikliui taip pat

buvo suteikiamas pastovus +0,2 V (vs Ag|AgCl, KCl_{sot.}) potencialas. Tarp tyrimų skirtingo pH PBS, biologinis jutiklis buvo regeneruojamas įmerkiant jį į PBS (pH 5,5) vienai minutei.

Optinio vandenilio peroksido jutiklio (glass|ITO|CoHCF_{ox}|KCl_{cycled} elektrodo) tyrimai

Glass|ITO|CoHCF_{ox}|KCl_{cycled} elektrodo atsakas į H₂O₂ buvo tiriamas skaidraus stiklo kiuvetėje, užpildytoje 0,5 M KCl tirpalu, į kurią buvo lašinamos įvairios (nuo 1,5 mM iki 20 mM) H₂O₂ koncentracijos. Glass|ITO|CoHCF_{ox}|KCl_{cycled} elektrodo absorbcijos spektrai registruoti praėjus 5 min. nuo H₂O₂ įlašavimo į 0,5 M KCl. Užregistravus absorbcijos spektrą tam tikrą H₂O₂ koncentraciją turinčiame KCl tirpale, jutiklio CoHCF sluoksnis buvo oksiduojamas atgal į pradinę CoHCF_{ox} būseną taikant ciklinę voltamperometriją: jutikliui suteikta 15 potencialo ciklų nuo +0,9 V iki +0,1 V (vs Ag|AgCl, KCl_{sot.}), naudojant 50,0 mVs⁻¹ potencialo skleidimo greitį.

Amperometrinio biologinio Hg²⁺ jonų jutiklio (glass|FTO|PB|GOx) tyrimai

Glass|FTO|PB|GOx biologinio jutiklio amperometrinis atsakas į Hg²⁺ jonus buvo tiriamas 1,3 mM gliukozės turinčiame PBS, į jį pridėdant įvairias (nuo 27 μM iki 247 μM) HgCl₂ koncentracijas. Šio biologinio jutiklio veikimas remiasi vandenilio peroksido redukcijos srovės sumažėjimo, vykstančio dėl GOx inhibicijos Hg²⁺ jonais, matavimu. Hg²⁺ jonų sukeliamas vandenilio peroksido redukcijos srovės sumažėjimas (dj, %) buvo įvertinamas panaudojant 1 lygtį [47]:

$$dj = \frac{I_0 - I_i}{I_0} \cdot 100\% \quad (1)$$

čia I_0 – redukcijos srovė, išmatuota po gliukozės (1,3 mM) pridėjimo į PBS; I_i – redukcijos srovė, išmatuota pridėjus Hg²⁺ jonų į 1,3 mM gliukozės turintį PBS.

REZULTATŲ APITARIMAS

ELEKTROCHROMINIO AMONIO JONŲ JUTIKLIO (glass|ITO|PB) TYRIMAI

Elektrocheminis Berlyno mėlynojo stabilizavimas

Siekiant elektrochemiškai stabilizuoti glass|ITO|PB elektrodo PB sluoksnį pervedant PB į K^+ jonais praturtintą formą ($KFe^{III}[Fe^{II}(CN)_6]$), šio darbo metu [65] buvo pritaikyta ciklinės voltamperometrijos procedūra 0,1 M KCl tirpale (1A pav., 27 psl.). Registruojant ciklines voltamperogramas, pirmųjų šešių voltamperinių ciklų metu stebėtas katodinės ir anodinės srovės pikų siaurėjimas, susijęs su K^+ jonais nepraturtintos PB formos virsmu į elektrochemiškai stabilesnę K^+ jonais praturtintą formą [3,7]. Norint patvirtinti PB virsmą į K^+ jonais praturtintą formą, šio tyrimo metu taip pat buvo registruojami glass|ITO|PB elektrodo absorbcijos spektrai prieš pritaikant ciklinės voltamperometrijos procedūrą (elektrochemiškai stabilizuojant PB dangą) ir po jos pritaikymo (1B pav., 27 psl.). Nustatyta, kad, elektrochemiškai stabilizavus PB dangą, optinės absorbcijos maksimumo vertė pasikeitė nuo 0,418 santykinų absorbcijos vienetų (u.a.) (prieš stabilizavimą), iki 0,499 u.a. (po stabilizavimo), o absorbcijos maksimumą atitinkantis bangos ilgis (λ_{max}) pasislinko nuo 720 nm iki 707 nm. Tokie patys efektai – absorbcijos maksimumo vertės padidėjimas ir absorbcijos maksimumą atitinkančio bangos ilgio poslinkis į trumpesnes bangas –, gaunami tiriant K^+ jonais nepraturtinto PB virsmą į K^+ jonais praturtintą formą, buvo aprašyti ir kitų autorių atliktuose tyrimuose [24,66]. Taigi, galima daryti išvadą, kad ciklinės voltamperometrijos procedūra 0,1 M KCl tirpale sėkmingai leido pervesti po nusodinimo gautą PB dangą į K^+ jonais praturtintą formą.

Glass|ITO|PB elektrodo ciklinės voltamperometrijos kreivėse (1A pav., 27 psl.) matoma, kad PB pusbangės potencialas yra +0,18 V (vs Ag|AgCl, $KCl_{sot.}$). Atsižvelgiant į tai, kad amonio jonų nulemti PB redokso virsmai turėtų būti geriausiai matomi tuomet, kai glass|ITO|PB elektrodai yra suteikiamas potencialas, artimas PB redukcijos potencialui, tolimesnių glass|ITO|PB elektrodo (jutiklio) tyrimų amonio jonų turinčiuose tirpaluose metu buvo nuspręsta suteikti elektrodai +0,2 V (vs Ag|AgCl, $KCl_{sot.}$) potencialą, kuris yra labai artimas +0,18 V.

Elektrochrominio amonio jonų jutiklio (glass|ITO|PB elektrodo) tyrimas amonio jonų turinčiuose tirpaluose

Glass|ITO|PB elektrodo elektrochrominio atsako į amonio jonus tyrimo metu nustatyta, kad glass|ITO|PB elektrodo absorbcijos maksimumo padėtis ir vertė priklauso nuo NH_4^+ jonų koncentracijos tirpale (2 pav., 28 psl.): NH_4^+ jonų koncentracijos tirpale padidėjimas lėmė absorbcijos maksimumo vertės sumažėjimą ir λ_{max} poslinkį į ilgesnes bangas. Šio tyrimo metu taip pat nustatyta, kad glass|ITO|PB elektrodo absorbcijos vertė ties 730 nm bangos ilgiu, taip pat ir λ_{max} vertė, tiesiškai priklauso nuo amonio jonų koncentracijos intervale nuo 0,01 M iki 0,1 M (2B ir 2C pav., 28 psl.).

Amonio jonų sukeltas glass|ITO|PB elektrodo absorbcijos sumažėjimas (2 pav., 28 psl.) yra galimai susijęs su elektrochrominiu PB virsmu į bespalvę redukuotą formą, Berlyno baltąjį (PW). Šią prielaidą pagrindžia anksčiau atlikti tyrimai [51], kuriuose teigiama, kad PB redukcijos potencialas priklauso nuo amonio jonų koncentracijos tirpale pagal Nernsto lygtį – padidėjus amonio jonų koncentracijai tirpale, padidėja ir PB redukcijos potencialas [51]. Taigi, suteikus glass|ITO|PB elektrodai pastovų +0,2 V (*vs* Ag|AgCl, KCl_{sat}) potencialą ir padidinant amonio jonų koncentraciją tirpale, dėl PB redukcijos potencialo padidėjimo vis daugiau PB kristalinių vienetų pereina į bespalvę PW formą, o tai nulemia PB dangos blukimą (2 pav., 28 psl.).

ELEKTROCHROMINIO BIOLOGINIO KARBAMIDO JUTIKLIO (Glass|ITO|PB|urease) TYRIMAI

Glass|ITO|PB|urease biologinio jutiklio tyrimas skirtingos koncentracijos karbamido tirpaluose

Fermentas ureazė yra plačiai naudojamas biologiniuose karbamido jutikliuose, kadangi ureazės katalizuojamos karbamido hidrolizės reakcijos metu kinta įvairūs elektrocheminiai ar kitais metodais išmatuojami faktoriai, tokie kaip pH, amonio jonų ir anglies dvideginio koncentracija, temperatūra [67,68]. Atsižvelgiant į elektrochrominio amonio jonų jutiklio (glass|ITO|PB) tyrimus, parodžiusius, kad glass|ITO|PB elektrodas yra tinkamas amonio jonų koncentracijos tirpale nustatymui (2 pav., 28 psl.), kai elektrodai suteikiamas +0,2 V (*vs* Ag|AgCl, KCl_{sat}) potencialas, buvo nutarta suformuoti elektrochrominį biologinį karbamido jutiklį, fiksuojant fermentą ureazę glass|ITO|PB elektrodo PB dangos paviršiuje (glass|ITO|PB|urease).

Glass|ITO|PB|urease biologinis jutiklis buvo tiriamas panašiomis sąlygomis, kaip ir prieš tai tirtas elektrochrominis amonio jonų jutiklis – pastovus +0,2 V (vs Ag|AgCl, KCl_{sat.}) potencialas buvo suteiktas glass|ITO|PB|urease jutikliui tiriant jį karbamido turinčiuose fosfatiniuose buferiniuose tirpaluose (PBS). Didėjant karbamido koncentracijai PBS, glass|ITO|PB|urease jutiklio absorbcija mažėjo (4 pav., 32 psl.), o tai yra numatoma susiję su amonio jonų sukelta PB redukcija į PW. Be to, karbamido pridėjimo sukeltas absorbcijos maksimumo sumažėjimas (ΔA) tiesiškai priklausė nuo karbamido koncentracijos PBS (5 pav., 32 psl.) koncentracijų intervale nuo 3 mM iki 30 mM. Apskaičiuotas glass|ITO|PB|urease biologinio jutiklio jautrumas karbamidui yra 4,2 u.a. M⁻¹. Glass|ITO|PB|urease jutiklio tyrimų metu gautas tiesinis koncentracijų intervalas (nuo 3 mM iki 30 mM) yra platesnis nei tiesinis koncentracijų intervalas, gautas kitų autorių atlikto [24] K⁺ jonais nepraturtinto PB šarminės hidrolizės principu veikiančio biologinio karbamido jutiklio tyrimo metu (nuo 2 mM iki 12 mM), tačiau abu šie tiesiniai koncentracijų intervalai (nuo 3 mM iki 30 mM ir nuo 2 mM iki 12 mM) apima normalios karbamido koncentracijos kraujyje viršutinę ribą (7,5 mM [58]).

Po tyrimo karbamido turinčiame PBS, glass|ITO|PB|urease biologinis jutiklis buvo regeneruojamas įmerkiant jį į karbamido neturintį PBS (pH 5,5) vienai minutei. Absorbcijos spektrai, išmatuoti prieš glass|ITO|PB|urease biologinio jutiklio tyrimą karbamido turinčiame PBS ir po jo regeneracijos, turėjo tą pačią formą (6 pav., 33 psl.), o tai rodo gerą regeneracijos procedūros efektyvumą. Glass|ITO|PB|urease biologinio jutiklio regeneracija PBS gali būti paaiškinama spontanine PW reoksidacija į PB deguonies turinčiuose tirpaluose [31,33,34].

pH įtakos glass|ITO|PB|urease biologinio jutiklio optinėms savybėms tyrimas

Yra žinoma [24,56,57], kad K⁺ jonais nepraturtinto PB optinės savybės priklauso nuo tirpalo pH. Tirpalo pH padidėjimas, atsirandantis vykstant ureazės katalizuojamai karbamido hidrolizei, sukelia PB dangos absorbcijos sumažėjimą dėl grįžtamosios K⁺ jonais nepraturtinto PB hidrolizės šarminėje terpėje [24,56,57]. Toks pats efektas (PB dangos absorbcijos sumažėjimas) buvo stebimas ir glass|ITO|PB elektrodo tyrimų metu, kuomet, suteikus elektrodai pastovų +0,2 V (vs Ag|AgCl, KCl_{sat.}) potencialą ir didinant amonio jonų koncentraciją tirpale, buvo stebimas PB dangos blukimas dėl elektrochrominio PB virsmo į PW (2 pav., 28 psl.). Taigi, siekiant patikslinti

glass|ITO|PB|urease biologinio jono atsako į karbamidą kilmę, šio darbo metu buvo tiriama pH įtaka glass|ITO|PB|urease biologinio jutiklio optinėms savybėms.

Buvo nustatyta, kad, 2 min. trunkančio glass|ITO|PB|urease biologinio jutiklio tyrimo 30 mM karbamido turinčiame PBS metu, PBS pH vertė (5,5) išlieka nepakitusi, o tai rodo gerą pasirinkto PBS buferinę talpą. Vis dėlto, ureazės katalizuojamos karbamido hidrolizės metu atsirandantis pH padidėjimas prie elektrochrominio PB sluoksnio gali būti didesnis, negu pH padidėjimas tirpalo dalyje, nutolusioje nuo jutiklio, o tai potencialiai gali sukelti PB absorbcijos intensyvumo sumažėjimą. Siekiant įvertinti pH įtaką glass|ITO|PB|urease biologinio jutiklio optinėms savybėms, glass|ITO|PB|urease jutiklis buvo ištirtas PBS su įvairiais pH (nuo 5,5 iki 12). Šio tyrimo metu glass|ITO|PB|urease jutikliui suteiktas pastovus +0.2 V (vs Ag|AgCl, KCl_{sat.}) potencialas, o absorbcijos spektrai registruoti palaikius glass|ITO|PB|urease jutiklį kiekvieno pH PBS 2 min. Nustatyta, kad, tiriant glass|ITO|PB|urease biologinį jutiklį PBS su pH verte nuo 5,5 iki 11, šio jutiklio absorbcijos spektras išlieka nepakitęs (7 pav., 36 psl.), tačiau, tiriant jutiklį pH 12 PBS, PB|urease danga atsilupo nuo glass|ITO|PB|urease elektrodo.

Biologinio jutiklio optinių savybių atsparumas pH vertės didėjimui pH intervale nuo 5,5 iki 11 gali būti susijęs su tuo, kad, formuojant glass|ITO|PB|urease biologinį jutiklį, buvo pasirinkta naudoti K⁺ jonais praturtintą PB (KFe^{III}[Fe^{II}(CN)₆]). Ankstesnių PB dangos optinių savybių priklausomybės nuo tirpalo pH tyrimų [24,56,57] metu buvo naudojami K⁺ jonais nepraturtinti PB sluoksniai, o tyrimų, kurių metu būtų pademonstruotas K⁺ jonais praturtinto PB optinis atsakas į pH pokyčius, kiek žinoma, nėra publikuota. Be to, PB|urease dangos atsilupimas nuo glass|ITO|PB|urease biologinio jutiklio negali būti laikomas biologinio jutiklio veikimo principu, kadangi šio darbo metu suformuotas jutiklis buvo sėkmingai regeneruojamas po tyrimo karbamido turinčiame PBS (6 pav., 33 psl.). Taigi, apibendrinant glass|ITO|PB|urease biologinio jutiklio tyrimo skirtingo pH PBS rezultatus galima daryti išvadą, kad vienintelis mechanizmas, paaiškinantis glass|ITO|PB|urease jutiklio atsaką į karbamidą, turėtų būti susijęs su elektrochrominiu PB virsmu į PW formą, kurį sukelia karbamido hidrolizės produktų – amonio jonų – koncentracijos padidėjimas tirpale. Be to, glass|ITO|PB|urease biologinio jutiklio nejautrumas pH pokyčiams gali padėti apeiti dažną PB optinio jautrumo pH pokyčiams principu veikiančių karbamido biologinių jutiklių problemą – biologinio jutiklio jautrumo karbamidui priklausomybę nuo mėginio buferio talpos [24].

OPTINIO JUTIKLIO, VEIKIANČIO KOBALTO HEKSACIANOFERATO JAUTRUMO VANDENILIO PEROKSIDUI PAGRINDU, TYRIMAI

Kobalto heksacianoferato elektrocheminių ir elektrochrominių savybių tyrimai

Kobalto heksacianoferato (CoHCF) struktūrinis analogas – Berlyno baltasis (PW) – gali būti pritaikomas optiniam vandenilio peroksido nustatymui: PW reaguoja su H_2O_2 ir šios reakcijos metu PW oksiduojasi į ryškiai mėlyną PB. Vis dėlto, PW pagrindo H_2O_2 jutikliai turi trūkumą – jų jautrumas H_2O_2 gali sumažėti dėl deguonies buvimo tirpale [31,32,34]. Be to, yra žinoma, kad CoHCF gali būti naudojamas kaip elektrocheminės H_2O_2 oksidacijos katalizatorius [37,38]. Taigi, CoHCF danga oksiduotame būvyje ($CoHCF_{ox}$) potencialiai gali būti panaudojama ir optiniam H_2O_2 nustatymui. Be to, $CoHCF_{ox}$, kaip oksidacinių savybių turintis junginys, turėtų būti atsparus oro deguonies, bei vandenyje ištirpusio deguonies poveikiui. Dėl šių priežasčių – potencialaus $CoHCF_{ox}$ pritaikomumo H_2O_2 detekcijai ir galimo atsparumo deguonies poveikiui – šio darbo metu buvo formuojamas optinis $CoHCF_{ox}$ pagrindo H_2O_2 jutiklis [70].

Prieš pritaikant $CoHCF_{ox}$ optiniam H_2O_2 nustatymui, CoHCF padengtas elektrodas (glass|ITO|CoHCF) buvo tiriamas ciklinės voltamperometrijos ir absorbcinės spektrinės analizės būdu, siekiant išsirinkti tinkamas sąlygas (KCl tirpalo koncentraciją) jutiklio veikimui. Glass|ITO|CoHCF elektrodo ciklinės voltamperometrijos tyrimo 0,5 M KCl tirpale metu buvo gautos voltampermetrinės kreivės, kurios išlaikė pastovią formą penkiolikos ciklinių potencialo skleidimų (nuo +0,9 V iki +0,1 V vs $Ag|AgCl, KCl_{sot.}$) metu (8A pav., 38 psl.). Be to, EDS analizė patvirtino, kad glass|ITO|CoHCF elektrodo CoHCF sluoksnis turi tą pačią formulę ($K_{1,2}Co_{1,1}[Fe(CN)_6]$) tiek prieš ciklinės voltamperometrijos eksperimentą 0,5 M KCl tirpale, tiek po jo [70]. Šie rezultatai rodo gerą CoHCF cheminį ir elektrocheminį stabilumą 0,5 M KCl tirpale.

Nors CoHCF danga pasižymėjo geru elektrocheminiu stabilumu 0,5 M KCl tirpale (8A pav., 38 psl.), glass|ITO|CoHCF elektrodo ciklinės voltamperometrijos tyrimų 0,1 M KCl tirpale metu buvo stebimas redokso smailių mažėjimas visų penkiolikos voltamperinių ciklų suteikimo metu (8B pav., 38 psl.). Šis smailių mažėjimas gali būti susijęs su po elektrocheminio nusodinimo gauto K^+ jonais praturtinto CoHCF ($K_{1,2}Co_{1,1}[Fe(CN)_6]$) virsmu į K^+ jonais nepraturtintą CoHCF formą, kadangi pastaroji forma yra

elektrochemiškai mažiau aktyvi [7]. Taigi, 0,1 M KCl koncentracija yra per maža nekintančioms CoHCF ($K_{1,2}Co_{1,1}[Fe(CN)_6]$) elektrocheminėms savybėms palaikyti.

Absorbcinės spektrinės analizės tyrimai parodė, kad CoHCF danga pasižymi didesniu absorbcijos vertės skirtumu tarp oksiduotos (CoHCF_{ox}) ir redukuotos (CoHCF_{red}) formų, kai absorbcijos spektrai registruojami 0,5 M KCl tirpale (gautas 0,085 u.a. skirtumas, 9A pav., 40 psl.), nei 0,1 M KCl tirpale (gautas 0,009 u.a. skirtumas, 9B pav., 40 psl.). Be to, CoHCF_{ox} spektro forma abejuose KCl tirpaluose (0,1 M ir 0,5 M) buvo panaši (9 pav., 40 psl.) ir iš to galima daryti prielaidą, kad CoHCF_{ox} virsmas į CoHCF_{red} 0,1 M KCl yra apsunkintas. Taigi, atsižvelgiant į geresnį CoHCF elektrocheminį stabilumą ir didesnę elektrocheminį virsmą registruotus 0,5 M KCl tirpale, šis tirpalas (0,5 M KCl) buvo pasirinktas tolimesniems CoHCF_{ox} pagrindo jutiklio atsako į H₂O₂ tyrimams.

Deguonies įtakos CoHCF_{ox} optinėms savybėms tyrimas

Siekiant nustatyti, ar oro deguonis turi įtakos CoHCF_{ox} optinėms savybėms, ciklinės voltamperometrijos 0,5 M KCl tirpale procedūra (8A pav., 38 psl.) paveiktas glass|ITO|CoHCF elektrodas (glass|ITO|CoHCF_{ox}|KCl_{cycled}) buvo laikomas kambario sąlygomis savaitę. Nustatyta, kad glass|ITO|CoHCF_{ox}|KCl_{cycled} elektrodo absorbcijos intensyvumas 7 dienų laikotarpyje nesumažėjo (10A pav., 42 psl.), taigi, CoHCF_{ox} nekeitė savo oksidacinės būsenos. Iš to galima daryti išvadą, kad CoHCF_{ox} yra atsparus deguonies poveikiui ir CoHCF_{ox} pagrindo jutiklis neturėtų prarasti savo jautrumo vandenilio peroksidui dėl sąveikos tarp CoHCF_{ox} ir deguonies.

Vandenilio peroksido jutiklio (glass|ITO|CoHCF_{ox}|KCl_{cycled} elektrodo) optinio atsako į vandenilio peroksidą tyrimas

Glass|ITO|CoHCF_{ox}|KCl_{cycled} elektrodo optinio atsako į H₂O₂ tyrimas atliktas pridėdant įvairias H₂O₂ koncentracijas (nuo 1,5 mM iki 20 mM) į 0,5 M KCl ir registruojant glass|ITO|CoHCF_{ox}|KCl_{cycled} elektrodo absorbcijos spektrą praėjus 5 min. nuo H₂O₂ įlašavimo į 0,5 M KCl. H₂O₂ įlašinimas į 0,5 M KCl sukėlė glass|ITO|CoHCF_{ox}|KCl_{cycled} elektrodo absorbcijos sumažėjimą (10B pav., 42 psl.), o tai numatomai yra susiję su H₂O₂ sukeltu CoHCF_{ox} virsmu į CoHCF_{red}. H₂O₂ sukeltą CoHCF_{ox} redukciją patvirtina ir sėkmingas CoHCF elektrocheminis oksidavimas atgal į pradinę (CoHCF_{ox}) būseną po tyrimo H₂O₂ turinčiame tirpale (10B pav., 42 psl.).

Šio darbo metu buvo nustatyta, kad H_2O_2 sukeltas glass|ITO|CoHCF_{ox}|KCl_{cycled} elektrodo absorbcijos sumažėjimas yra tiesiškai priklausomas nuo H_2O_2 koncentracijos intervale nuo 1,5 mM iki 20 mM (11 pav., 43 psl). Apskaičiuotas glass|ITO|CoHCF_{ox}|KCl_{cycled} elektrodo jautrumas H_2O_2 yra 0,82 u.a. M⁻¹. Palyginimo dėlei, ankstesnių tyrimų metu sukurti elektrocheminiai CoHCF pagrindo H_2O_2 jutikliai pasižymėjo tiesiniais intervalais su 7 nM – 700 nM apatinėmis ir 1,2 – 9,0 mM viršutinėmis H_2O_2 koncentracijų ribomis [37,38]. Taigi, šio darbo metu suformuotas optinis H_2O_2 jutiklis (glass|ITO|CoHCF_{ox}|KCl_{cycled} elektrodas) yra tinkamesnis didesnių koncentracijų nustatymui, nei elektrocheminiai CoHCF pagrindo H_2O_2 jutikliai [37,38].

AMPEROMETRINIO BIOLOGINIO Hg^{2+} JONŲ JUTIKLIO (Glass|FTO|PB|GOx) TYRIMAI

Glass|FTO|PB|GOx biologinio jutiklio veikimo principas

Hg^{2+} jonai yra žinomi gliukozės oksidazės (GOx) inhibitoriai [44,46,47]. Glass|FTO|PB|GOx biologinio jutiklio veikimo metu [74] į PBS buvo pridėdama gliukozės, kad vyktų GOx katalizuojama gliukozės oksidacijos reakcija, kurios metu išsiskiria H_2O_2 , kuris elektrochemiškai redukuojasi jutiklio paviršiuje dėl PB elektrokatalitinių savybių [10,19,40]. Tačiau, į gliukozės turintį PBS pridėjus Hg^{2+} , vyko GOx inhibicija, dėl kurios buvo stebimas H_2O_2 redukcijos srovės sumažėjimas, leidęs kiekybiškai įvertinti Hg^{2+} koncentraciją tirpale (12 pav., 44 psl.).

Potencialo, optimalaus glass|FTO|PB|GOx biologinio jutiklio veikimui, parinkimas

Siekiant pritaikyti glass|FTO|PB|GOx biologinį jutiklį Hg^{2+} jonų nustatymui, svarbu parinkti potencialą, optimalų šio jutiklio veikimui. Glass|FTO|PB|GOx biologiniam jutikliui užduodamas potencialas turi būti: i) pakankamai žemas, kad vyktų PB katalizuojama H_2O_2 redukcijos reakcija ir ii) pakankamai aukštas, kad nevyktų elektrocheminė Hg^{2+} jonų redukcija. Ankstesnių tyrimų metu buvo nustatyta, kad PB pasižymi elektrokatalitiniu aktyvumu H_2O_2 redukcijos reakcijoje tuomet, kai yra perversas į redukuotą formą – PW [10,36,71,72]. Tam, kad PB danga būtų perversa į PW būvį, priklausomai nuo tirpalo ir PB danga padengto elektrodo

prigimties, PB padengtam elektrodai reikia suteikti potencialą, ne aukštesnį nei +0,15 V – +0,27 V vs Ag|AgCl, KCl_{sot.} [10,36,71,72]. Taigi, šio darbo metu, optimalių potenciostatinių sąlygų parinkimui, glass|FTO|PB elektrodas buvo amperometriškai tiriamas PBS, į kurią buvo pridėdama H₂O₂ (0,3 mM) ir Hg²⁺ (0,3 mM) jonų, kartu suteikiant glass|FTO|PB elektrodai +0,15 V, +0,20 V arba +0,25 V (vs Ag|AgCl, KCl_{sot.}) potencialą (13 pav., 44 psl.). Amperometrinių tyrimų metu buvo nustatyta, kad +0,15 V ir +0,25 V (vs Ag|AgCl, KCl_{sot.}) potencialai yra netinkami biologinio jutiklio veikimui: suteikus glass|FTO|PB elektrodai +0,15 V potencialą, buvo stebima Hg²⁺ jonų redukcija (13A pav., 46 psl.), o suteikus glass|FTO|PB elektrodai +0,25 V potencialą, buvo registruojama santykinai maža H₂O₂ redukcijos srovė (13B pav., 46 psl.). Tačiau, suteikus glass|FTO|PB elektrodai +0,20 V potencialą, buvo registruojama gana didelė (~ -50 μA cm²) H₂O₂ redukcijos srovė, o Hg²⁺ jonų pridėjimas nesukėlė jokio amperometrinio signalo (13C pav., 44 psl.), todėl +0,20 V potencialas buvo naudojamas ir tolimesnių glass|FTO|PB|GOx biologinio jutiklio atsako į skirtingas Hg²⁺ jonų koncentracijas tyrimų metu.

Amperometrinis glass|FTO|PB|GOx biologinio jutiklio tyrimas

Amperometrinis glass|FTO|PB|GOx biologinio jutiklio tyrimas buvo atliktas PBS tirpale, suteikiant glass|FTO|PB|GOx biologiniam jutikliui +0,2 V (vs Ag|AgCl, KCl_{sot.}) potencialą. Tyrimo metu į PBS buvo lašinama gliukozė (1,3 mM), o vėliau – Hg²⁺ jonai (nuo 27 μM iki 247 μM). Gliukozės pridėjimas į PBS sukeldavo katodinės srovės augimą, o Hg²⁺ jonų pridėjimas sukeldavo katodinės srovės sumažėjimą (14A pav., 48 psl.). Šio tyrimo metu taip pat nustatyta, kad, ištyrus glass|FTO|PB|GOx biologinį jutiklį Hg²⁺ jonų ir gliukozės turinčiame PBS bei regeneravus jutiklį 0,1 M etilendiamintetraacto rūgšties (EDTA) tirpalu [74], biologinio jutiklio amperometrinis atsakas į gliukozę (1,3 mM) sumažėjo ~ 28 %. Dėl šios priežasties, vienas glass|FTO|PB|GOx biologinis jutiklis buvo tiriamas tik vienos Hg²⁺ jonų koncentracijos tirpale, t. y. kas kartą atliekant tyrimą kitokios Hg²⁺ jonų koncentracijos tirpale, buvo naudojamas naujas glass|FTO|PB|GOx biologinis jutiklis. Nustatyta, kad Hg²⁺ jonų pridėjimo į gliukozę turintį PBS sukėlė katodinės srovės sumažėjimą (dj, %), tiesiškai proporcingą Hg²⁺ jonų koncentracijai intervale nuo 27 μM iki 247 μM (14B pav., 48 psl.). Palyginimo dėlei, kitų autorių tirti amperometriniai GOx inhibicijos pagrindu veikę Hg²⁺ jonų jutikliai pasižymėjo tiesiniais koncentracijų intervalais, varijuojančiais tarp 0,025 μM ir 180 μM (lentelė 2, 49 psl.) Taigi, šio darbo

metu suformuotas biologinis Hg^{2+} jonų jutiklis, palyginus su kitais GOx inhibicijos principu veikiančiais amperometriniais Hg^{2+} jonų jutikliais, gali būti pritaikomas didesnių Hg^{2+} koncentracijų nustatymui, o tai yra naudinga tiriant mėginius, turinčius dideles Hg^{2+} jonų koncentracijas (pvz.: dirvos ir nuosėdų ekstraktus [77-80]). Vis dėlto, bene didžiausias glass|FTO|PB|GOx biologinio jutiklio pranašumas, lyginant jį su kitais GOx inhibicijos principu veikiančiais amperometriniais biologiniais Hg^{2+} jonų jutikliais, yra tai, kad glass|FTO|PB|GOx jutiklis veikė suteikus jam sąlyginai (lentelė 2, 49 psl.) žemą (+0,2 V vs Ag|AgCl, $\text{KCl}_{\text{sat.}}$) potencialą, o tai padeda išvengti tam tikrų pašalinių reakcijų (pvz.: alkilfenolių arba sulfitų oksidacijos [48,49,50]), kurios gali sumažinti analizės patikimumą.

IŠVADOS

1. Berlyno mėlynasis buvo pritaikytas formuojant elektrochrominį amonio jonų jutiklį (glass|ITO|PB). Glass|ITO|PB jutiklis pasižymėjo tiesiniu koncentracijų intervalu nuo 0,01 M iki 0,1 M bei 0,35 u.a. M^{-1} jautrumu.
2. Elektrochrominis karbamido jutiklis buvo suformuotas padengiant glass|ITO elektrodą Berlyno mėlynojo sluoksniu (glass|ITO|PB) ir fiksuojant fermentą ureazę glass|ITO|PB elektrodo Berlyno mėlynojo dangos paviršiuje (glass|ITO|PB|urease). Glass|ITO|PB|urease jutiklis pasižymėjo tiesiniu koncentracijų intervalu nuo 3 mM iki 30 mM bei 4,2 u.a. M^{-1} jautrumu.
3. Kobalto heksacianoferatas buvo pritaikytas formuojant optinį vandenilio peroksido jutiklį (glass|ITO|CoHCF_{ox}|KCl_{cycled}). Glass|ITO|CoHCF_{ox}|KCl_{cycled} jutiklis pasižymėjo tiesiniu koncentracijų intervalu nuo 1,5 mM iki 20 mM bei 0,82 u.a. M^{-1} jautrumu.
4. Amperometrinis biologinis Hg^{2+} jonų jutiklis buvo suformuotas padengiant glass|FTO elektrodą Berlyno mėlynojo sluoksniu (glass|FTO|PB) ir fiksuojant fermentą gliukozės oksidazę nusodintos Berlyno mėlynojo dangos paviršiuje (glass|FTO|PB|GOx). Glass|FTO|PB|GOx jutiklis pasižymėjo tiesiniu koncentracijų intervalu nuo 27 μM iki 247 μM .

ACKNOWLEDGEMENT

I sincerely thank my supervisor Prof. Dr. Aušra Valiūnienė for guidance during doctoral studies, help in strengthening skills in electrochemistry and for shared knowledge of planning experiments and writing scientific publications.

I also thank Prof. (HP) Dr. Arūnas Ramanavičius for his help in generating ideas for experiments and for all advices in writing scientific publications.

Special thanks to Prof. Dr. Valentina Plaušinitienė for her help with XRD and SEM investigations.

Finally, I would like to thank the entire Department of Physical Chemistry and our laboratory team for their help, especially Gabija Kavaliauskaitė, Gerda Žižiūnaitė, Narvydas Dėnas, Diana Baryševa and Giedrė Medvikytė.

CURRICULUM VITAE

PERSONAL INFORMATION

Name, Surname Povilas Virbickas
Mobile + 370 620 29 079
E-mail povilas.virbickas@chgf.vu.lt
Date of birth 1993 10 16

EDUCATION

Date 2017 – 2019
University Vilnius University
Study programme Biochemistry
Degree awarded Master of Biochemistry

Date 2013 – 2017
University Vilnius University
Study programme Nanotechnologies and Material Science
Degree awarded Bachelor of Chemistry

WORK EXPERIENCE

Date 2019 10 – now
Institution Vilnius University, Faculty of Chemistry and Geosciences
Position Junior assistant

Date 2018 08 – 2020 08
Institution Environmental Protection Agency
Position Chief Specialist

Date 2017 08 – 2018 08
Institution Environmental Protection Agency
Position Senior Specialist

INTERNSHIPS

ERASMUS+ internship “Preparation and electrochemical investigation of human skin-simulating structures”, Malmo University, Sweden (2022-06-01 – 2022-09-01).

Vilniaus universiteto leidykla
Saulėtekio al. 9, III rūmai, LT-10222 Vilnius
El. p. info@leidykla.vu.lt, www.leidykla.vu.lt
bookshop.vu.lt, journals.vu.lt
Tiražas 15 egz.